New genomic resources and toolkits for developmental study of whip spiders (Amblypygi) provide insights into arachnid genome evolution and antenniform leg patterning

Guilherme Gainett[1], Prashant P. Sharma[1]

[1]Department of Integrative Biology, University of Wisconsin-Madison, Madison, WI, USA 53706

Correspondence: guilherme.gainett@wisc.edu

Abstract

The resurgence of interest in the comparative developmental study of chelicerates has led to important insights, such as the discovery of a genome duplication shared by spiders and scorpions, inferred to have occurred in the newly proposed clade Arachnopulmonata. Nonetheless, several groups remain understudied in the context of development and genomics, such as the order Amblypygi (whip spiders). The phylogenetic position of Amblypygi in Arachnopulmonata poses them as an interesting group to test the extent of conservation of the proposed genome duplication in the history of arachnids. Moreover, whip spiders have their first pair of walking legs elongated and modified into sensory appendages (a convergence with the antenna of mandibulates), but the genetic patterning of these antenniform legs has never been investigated. Here, we break a 45-year hiatus of embryological studies in Amblypygi, by establishing genomic resources and protocols for cultivation of embryos and gene expression assays by in situ hybridization to study the development of the whip spider *Phrynus marginemaculatus*. We provide evidence that *P. marginemaculatus* retains duplicates of most Hox genes, and that paralogs of the leg gap genes *dachshund* and *homothorax* retain arachnopulmonate-specific expression patterns. We characterize the expression of leg gap genes *Distal-less*, *dachshund1/2* and *homothorax1/2* in the embryonic antenniform leg and other appendages, and provide evidence that allometry, and by extension the antenniform leg fate, is already specified very early in embryogenesis.

Keywords: Arachnopulmonata; gene duplication; paralogs; leg gap genes; sensory biology

Introduction

In the past 25 years, comparative developmental study of chelicerates has resurged with the integration of molecular biology and genomics, spearheaded by developmental genetic investigations of the spiders *Cupiennius salei* and *Parasteatoda tepidariorum* (Akiyama-Oda & Oda, 2003; 2010; W. G. M. Damen, Hausdorf, Seyfarth, & Tautz, 1998; Schwager, Schoppmeier, Pechmann, & Damen, 2007; Schwager et al., 2017; Stollewerk, Schoppmeier, & Damen, 2003). Such works have revealed several important aspects of chelicerate development, such as the molecular mechanism of dorso-ventral axis patterning (Akiyama-Oda & Oda, 2003; 2006; Oda & Akiyama-Oda, 2008; Pechmann, Benton, Kenny, Posnien, & Roth, 2017), segmentation of the prosoma (Damen et al., 1998; Paese, Schoenauer, Leite, Russell, & McGregor, 2018; Pechmann et al., 2011; Schwager, Pechmann, Feitosa, McGregor, & Damen, 2009; Setton & Sharma, 2018) and opisthosoma (Paese et al., 2018; Stollewerk et al., 2003), and specification of prosomal versus opisthosomal fate (Khadjeh et al., 2012; Pechmann, Schwager, Turetzek, & Prpic, 2015). A few non-spider chelicerate models have also emerged in recent years and provided new perspectives on chelicerate development, such as the the horseshoe crab *Limulus polyphemus* (Xiphosura) (Blackburn et al., 2008; Mittmann & Scholtz, 2001) , the mites *Archegozetes longisetosus* (Barnett & Thomas, 2012; 2013a; 2013b; Telford & Thomas, 1998) and *Tetranychus urticae* (Acariformes) (Dearden, 2002; Grbić et al., 2007; Khila & Grbić, 2007a), the tick *Rhipicephalus microplus* (Parasitiformes) (Santos et al., 2013), the Arizona bark scorpion *Centruroides sculpturatus* (Sharma, Schwager, Extavour, & Wheeler, 2014b) (Scorpiones) and the harvestmen *Phalangium opilio* (Opiliones) (Sharma, Schwager, Extavour, & Giribet, 2012a; 2012b; Sharma, Schwager, Giribet, Jockusch, & Extavour, 2013; Sharma et al., 2015b). For instance, studies in *A. longisetosus* and *C. sculpturatus* have suggested that changes in Hox gene number and expression domains are responsible for both reduced segmentation of mites and the unique body plan of scorpions (Barnett & Thomas, 2013a; Sharma, Schwager, Extavour, & Wheeler, 2014b).

In addition to the insights into chelicerate development, one of the major recent outcomes of increasing availability of genomic resources in in the group was the discovery of a whole or partial genome duplication in spiders and scorpions. This genome duplication is inferred to trace back to the most recent common ancestor spiders and scorpions, the newly proposed clade Arachnopulmonata that includes all arachnid orders with book lungs (Leite et al., 2018; Schwager et al., 2017; Sharma, Kaluziak, Pérez-Porro, González, Hormiga, et al., 2014a; Sharma, Santiago, González-Santillán, Monod, & Wheeler, 2015a; Sharma,

Schwager, Extavour, & Wheeler, 2014b). This duplication event is also inferred to be independent from the multiple rounds of whole genome duplication undergone by horseshoe crabs (Xiphosura) (Kenny et al., 2015; Shingate et al., 2020). The duplication in spiders and scorpions encompasses several important developmental genes, such as the homeobox family (Leite et al., 2018; Schwager et al., 2017). Excitingly, there is increasing evidence of divergent expression and function of paralogs, such as in the case of Hox genes, leg gap genes and Retinal Determination Gene Network homologs (Gainett et al., 2020; Samadi, Schmid, & Eriksson, 2015; Schomburg, Turetzek, & Prpic, 2020; Schwager et al., 2017; Sharma, Schwager, Extavour, & Wheeler, 2014b; Turetzek, Khadjeh, Schomburg, & Prpic, 2017; Turetzek, Pechmann, Schomburg, Schneider, & Prpic, 2015).

Nevertheless, knowledge on the development of several arachnid orders still remains scarce or entirely unexplored in the contexts of embryological study and genomic architecture. One particularly interesting arachnid order whose genomic evolution and developmental biology remains largely unexplored is Amblypygi. Commonly known as whip spiders, Amblypygi comprise approximately 150 described species of nocturnal predators that are world-wide distributed primarily on the tropics and subtropics (Harvey, 2013; Weygoldt, 2000). Amblypygi is part of the clade Pedipalpi (together with the orders Thelyphonida and Schizomida), which in turn is sister group to spiders (Araneae) (Ballesteros & Sharma, 2019; Giribet, 2018; Lozano-Fernandez et al., 2019; Sharma, Kaluziak, Pérez-Porro, González, Hormiga, et al., 2014a). Considering the phylogenetic position of Amblypygi within Arachnopulmonata, a better understanding of Amblypygi genomics is anticipated to facilitate exploration of the evolutionary outcomes of genome duplication in Arachnopulmonata, and better characterizing the extent to which arachnopulmonate orders retained and specialized the ensuing paralogous genes. Unfortunately, the embryology of the order Amblypygi is known only from the works of Pereyaslawzewa (1901) a brief mention in Strubell (1892) ("Phrynidae"), Gough (1902), and the comprehensive study of Weygoldt (1975) in *Phrynus marginemaculatus* (formerly *Tarantula marginemaculata*).

Beyond the interest in their genomic architecture, whip spiders possess a fascinating biology and natural history. Whip spiders are emerging as model organisms in behavioral ecology, learning and neurophysiology in arachnids (Chapin & Hebets, 2016; Wiegmann et al., 2016). Their pedipalps, the second pair of appendages, are robust raptorial devices used for striking prey, including mostly arthropods, and even small vertebrates (Chapin & Hebets, 2016;

Seiter, Lemell, Gredler, & Wolff, 2019; Weygoldt, 2000). However, their most conspicuous characteristic and namesake is their "whip", a modified antenniform first walking leg that is not used for locomotion, but instead as a sensory appendage. The antenniform legs are extremely elongated relative to the other leg pairs, and the tibia and tarsus are pseudo-segmented into hundreds of articles that harbor an array of chemo-, thermo-, hygro- and mechanoreceptive sensilla (Igelmund, 1987; Foelix et al., 1975; Santer & Hebets 2011). The peripheral circuitry of the antenniform legs is complex, exhibiting peripheral synapses and giant neurons which are possibly involved in fast sensory responses (Foelix & Troyer, 1980; Santer & Hebets, 2011). The antenniform legs also have been shown to be important for foraging, mating, and intrasexual contests (Santer & Hebets, 2008; 2011). Notably, concentration of sensory structures, elongation and pseudo-segmentation of these legs constitute a striking convergence with the antenna of mandibulate arthropods (Pancrustacea and Myriapoda). Evidence from Hox gene expression and functional experiments support the view that the antenna of mandibulates is positionally homologous to the chelicera of chelicerates (deutocerebral appendage) (Sharma et al., 2015b; Telford & Thomas, 1998). Despite their different positions along the antero-posterior axis of the body, the serial homology of antennae (mandibulates) and antenniform legs (whip spiders) to walking legs constitutes a potentially useful comparison to address whether a striking morphological convergence is associated with convergence in mechanisms of genetic patterning.

Most of the knowledge about the genetics of antenna versus leg fate specification in arthropods was discovered in the fruit fly *Drosophila melanogaster* and involves the regulation by leg gap genes and Hox genes. Broadly overlapping domains of leg gap genes *homothorax* (*hth*), *dachshund* (*dac*) and *Distal-less* (*Dll*) in the antenna promote antennal fate through activation of downstream antennal determinants such as *spineless* (Casares & Mann, 1998; Dong, Dicks, & Panganiban, 2002; Dong, Chu, & Panganiban, 2001; D. M. Duncan, Burgess, & Duncan, 1998; reviewed by Setton et al., 2017); leg identity in thoracic appendages is mediated by mutually antagonistic *hth* (proximal), *dac* (median) and *Dll* (distal) domains, and repression of *hth* by the Hox gene *Antennapedia* (*Antp*) (Casares & Mann, 1998; Struhl, 1981; 1982). Ectopic expression of *hth* on the leg discs results in leg-to-antenna transformation, whereas ectopic *Antp* in the antennal disc results in antenna-to-leg transformation (Casares & Mann, 1998; Struhl, 1981; 1982). In chelicerates, similar to *D. melanogaster*, the chelicera (antennal positional homolog) has broadly overlapping domains of *Dll* and *hth*; legs and pedipalps lack a distal *hth*, and a proximal *Dll* expression domain,

indicating a conservation of expression of positional homologs (Pechmann & Prpic, 2009; Prpic, Janssen, Wigand, Developmental, 2003, n.d.; Prpic & Damen, 2004; Sharma, Schwager, Extavour, & Giribet, 2012a). In line with this evidence, knockdown of *hth* in the harvestmen *Phalangium opilio* results in chelicera-to-leg transformation (and also partial pedipalp-to-leg transformation) (Sharma et al., 2015b). In contrast to *D. melanogaster* and other insects, arachnid *Antp* is not expressed on the leg-bearing segments, and knockdown of this gene in the spider *Parasteatoda tepidariorum* has revealed a role in repressing limbs in the opisthosoma (Khadjeh et al., 2012). Expression of *dac* in a mid-domain of chelicerate pedipalps and legs suggests a conserved role in mid segment patterning, and, accordingly, knockdown of *dac* in the harvestmen *P. opilio* and the spider *P. tepidariorum* results in defects on the mid-leg segments (Sharma et al., 2013; Turetzek et al., 2015). Additionally, loss of a *dac* domain of the chelicera of spiders in comparison to harvestman has been implicated in the transition from three- to two-segmented chelicera (Sharma et al., 2013; Sharma, Schwager, Extavour, & Giribet, 2012a).

Towards revitalizing embryological studies in Amblypygi, we generated herein protocols and comprehensive genomic resources for developmental genetic study of the whip spider *Phrynus marginemaculatus*, toward resuming the seminal studies begun by Peter Weygoldt with this promising model species. Leveraging a comprehensive developmental transcriptome for this species, and as a first step towards elucidating the patterning of antenniform legs, we characterized the expression pattern of the leg gap genes *homothorax*, *dachshund* and *Distal-less* in developing embryonic stages of *P. marginemaculatus* using newly established procedures for colorimetric whole mount in situ hybridization.

Methods

Establishment of amblypygid colony in the laboratory

Adult individuals of *Phrynus marginemaculatus* were purchased from a commercial supplier collects animals in the Florida Keys (USA). The maintenance of a colony of *Phrynus marginemaculatus* (Fig. 1A) in the laboratory followed guidelines provided is the original developmental works of Peter Weygoldt (Weygoldt, 1969; 1970; 1975) and notes on behavioral studies on this species (Fowler-Finn & Hebets, 2006; Rayor & Taylor, 2006; Santer & Hebets, 2009).While most species of Amblypygi have been reported as aggressive

and better kept in separate containers (Weygoldt, 2000), individuals of *P. marginemaculatus* can be keep in a stable laboratory colony in communitarian large containers (Rayor & Taylor, 2006). A maximum of 20 animals can be allowed to interact and mate freely in plastic boxes (67.3 x 41.9 x 32.4 cm) with a 2 cm layer of damp coconut fiber saturated with distilled water. The substrate is continuously dampened with approximately 500 mL of dH_2O on the substrate every week. All animals are keep in an acclimatized room at 26-28˚C in a controlled reversed 16L:8D light cycle to simulate summer months in Florida. To prevent flies from reproducing in this humid environment, the lid of the container is provided with a 10 x 20 cm fine mesh cloth, which also allows for air circulation. Each container is furnished with pieces of tree bark, egg carton, and retreats made from polystyrene foam or florist's foam, to provide enough space for animals to hide and suspend themselves during molting and egg-laying. After about two weeks of setting up a terrarium, the substrate hosted a stable colony of collembolans (possibly brought by the tree bark). The co-occurrence of collembolans does not appear to be disadvantageous in any way. Collembolans are invariably observed feasting on carcasses and likely contribute to preventing mite infestations (see also Weygoldt 2000). Animals are fed at least twice a week with nymphs of *Acheta domestica ad libitum*. Carcasses are removed as soon as detected to prevent the spread of mites. Freshly hatched praenymphs are kept with the female, and aggregate on the back of the brooding female (Fig. 1B). The next instar, the protonymph, disperse from the female upon molting. Protonymphs are transferred to communitarian terraria as described above. Protonymphs and subsequent instars until adulthood are fed pinheads of *A. domestica* and *Gryllus bimaculatus ad libitum* three times per week. The first adult individuals from our laboratory bred animals were detected 8 months after hatching, which accords to what has been described by Weygoldt (1975).

Terraria with adults are inspected daily for freshly molten individuals or ovigerous females, which are immediately separated from the main colony to avoid aggressive interactions. Ovigerous females carry the eggs outside the body in a brood sac attached to the ventral side of the opisthosoma (Weygoldt, 2000). Eggs are allowed to develop with the female until the desired stage for developmental work. Approximate stages may be inferred from days after egg laying (dAEL) at 26˚C following the staging in Weygoldt (1975). For obtaining the eggs, females are anesthetized with CO_2 and immobilized in customized plastic petri dishes (35 x 11 mm) with a central whole and foam (Fig. 1 C–D). With a blunt forceps pair, the pleura of the opisthosoma embracing the eggs may be gently displaced from the broodsac, and the

brood sac removed as whole (Fig. 1E). The female may be returned to the colony unharmed. The brood sac easily dismantles when immersed in a phosphate buffer solution (PBS), and eggs may be cleaned with forceps under PBS. We obtained high mortality in keeping isolated eggs developing in petri dishes with humid (wet filter paper) or dry in 26˚C incubators, as mold frequently develops. However, we found out that embryos will survive and develop immersed in PBS supplemented with kanamycin (1:5000) at 26˚C incubator and even hatch into deutembryos (~20 dAEL).

Phrynus marginemaculatus transcriptome assembly

We collected embryos of different embryonic stages as described above, and conducted total RNA extractions of each stage separately: hatched deutembryo (female #5, n=3; undetermined age, before eyespots), unhatched deutembryo (female #2 n=3; approx. 21 dAEL), and leg elongation stage (female #3, n=2; approx. 16-17 dAEL), late limb bud stage (female 6, n=1; 16 dAEL) and early limb bud stage (female 6, n=1; 14 dAEL) (voucher pictures are available upon request). Embryos were homogenized in Trizol TRIreagent (Invitrogen) and stored at –80˚C until extraction. The combined total RNA of the five extractions was submitted to cDNA library preparation and sequencing in an Illumina High-Seq platform using paired-end short read sequencing strategy (2 × 100 bp) at the Center for Gene Expression, Biotechnology Center of University of Wisconsin-Madison (USA). The quality of the raw reads was accessed assessed with FastQC (Babraham Bioinformatics). De novo assembly of compiled paired-end reads was conducted with the software Trinity v. 2.6.6 (Grabherr et al., 2011), using Trimmomatic v. 0.36 (Bolger, Lohse, & Usadel, 2014) to removed low quality reads and adaptors. Completeness of the transcriptome was assessed with the Trinity script '*TrinityStats.pl*', and BUSCO v. 3 (Waterhouse et al., 2017) on the longest isoforms using the database 'Arthropoda' and analysis of Hox genes. Whole transcriptome annotation was conducted following the Trinotate pipeline, by predicting proteins with TransDecoder v. 5.2.0 (Bryant et al., 2017) and searching best hits with blastx and blastp against Swiss-Prot and Pfam databases (The UniProt Consortium, 2018).

Gene identification

Hox genes (*labial*, *proboscipedia*, *Hox3*, *Deformed*, *Sex combs reduced*, *fushi tarazu*, *Antennapedia*, *Ultrabithorax*, *abdominal A* and *Abdominal B*), *Distal-less*, and *dachshund* orthologs were identified from the embryonic transcriptome of *Phrynus marginemaculatus* using BLAST searches (tblastn) with peptide queries of the homologs of *Drosophila melanogaster* and *Parasteatoda tepidariorum*. The best hits were reciprocally blasted to NCBI database and further assessed with a phylogenetic analysis.

For the phylogenetic analysis of Hox genes, we selected arthropod terminals with available genomes and well annotated references: the fruit fly *Drosophila melanogaster* (FlyBase), the beetle *Tribolium castaneum* (GCA_000002335.3) (Insecta), the centipede *Strigamia maritima* (GCA_000239455.1) (Myriapoda), the tick *Ixodes scapularis* (GCA_002892825.2), the mite *Tetranychus urticae* (GCA_000239435.1), the spider *Parastetoda tepidarioum* (GCA_000365465.2) and the scorpion *Centruroides sculpturatus* (GCA_000671375.2) (Chelicerata) (Chipman et al., 2014; Grbić et al., 2011; Gulia-Nuss et al., 2016; Herndon et al., 2020; Schwager et al., 2017) (Table S1). For the analysis of *Distal-less*, *dachshund*, and *homothorax* we selected terminals used in Nolan et al. (2020) (Nolan, Santibáñez López, & Sharma, 2020) and included the peptide sequence for *P. marginemaculatus* candidates (Table S1). Peptides were predicted with ORF Finder (NCBI) and TransDecoder v. 5.5.0 (Bryant et al., 2017) or obtained as CDS when possible from publicly available NCBI database. Peptide sequences were aligned using Clustal Omega (Sievers et al., 2011)in the software SeaView v. 4 (Gouy, Guindon, & Gascuel, 2010). Gene trees were inferred under maximum likelihood using IQTREE (Nguyen, Schmidt, Haeseler, & Minh, 2015)with automatic model selection (-m TEST) and 1000 ultrafast bootstrap resampling (-bb 1000).

Fixation and in situ hybridization

Collecting freshly laid eggs and keeping them in controlled temperature with the female or incubator (26˚C) allows to select desirable stages for fixation. We fixed embryos for in situ hybridization with three methods: (1) intact eggs in a phase of 4% formaldehyde/PBS and heptane overnight, after an established spider fixation protocol (Akiyama-Oda & Oda, 2003); (2) piercing a hole in the vitelline membrane, and immersing eggs in 4% formaldehyde/PBS overnight; (3) dissecting the embryo out of the vitelline membrane and fixing in 4% formaldehyde/PBS for periods varying from 2–24h. All three procedures were conducted in a shaking platform at room temperature (~22 ˚C). Following the fixation period, embryos were

rinsed several times in 1x PBS/0.1% Tween-20 (Sigma Aldrich) (PBS-T), and gradually dehydrated into pure methanol. Embryos may then be stored in 20 ˚C freezer until next procedures.

cDNA was synthetized with SuperScriptIII kit (Thermo Fisher) following the manufacturer's instructions, using the same total RNA used to generate the embryonic transcriptome. Riboprobe templates for the genes *Pmar-dac1*, *Pmar-dac2*, *Pmar-hth1*, and *Pmar hth-2* in situ hybridizations were generated as follows: genes were PCR amplified from cDNA using gene-specific primers designed with Primer3 v. 4.1.0 (Koressaar & Remm, 2007) and complemented with T7 linker sequences (5′ -ggccgcgg-3′ ; 5′ - cccggggc-3′), and a second PCR using universal T7 primer to generate T7 polymerase templates specific for sense (control) and anti-sense (signal) probes (Table S2). Sense and antisense riboprobes for *Pmar-Dll* were generated with T7 and T3 polymerases using a plasmid template. For cloning of *Pmar-Dll*, gene-specific primers were used to amplify an 848 bp fragment (Table S2), which was incorporated to vectors and *E. coli* using TOPO TA cloning kit (Thermo Fisher) following the manufacturer's instructions, and Sanger sequenced to confirm their identities.

For colorimetric in situ hybridization, we adapted a protocol for the spider *Parasteatoda tepidariorum* after Akiyama-Oda and Oda (2003). The staining reactions lasted between 2h and 8h at room temperature using nitro-blue tetrazolium (NBT) and 5-bromo-4-chloro-3′-indolyphosphate (BCIP) staining reactions (Sigma Aldrich). Embryos were then rinsed in PBS-T (0.05% Tween-20), counter-stained with 10µg/mL Hoechst 33342 (Sigma-Aldrich, St. Louis, MO, USA), post-fixed in 4% formaldehyde/PBS-T and stored at 4˚C. Images were taken in a petri dish with agar under PBS-T, using a Nikon SMZ25 fluorescence stereomicroscope mounted with either a DS-Fi2 digital color camera (Nikon Elements software). Appendage mounts were imaged in 70% glycerol/PBS-T in a Zeiss LCM 710 confocal microscope.

Results

Overview of embryogenesis in Amblypygi

A characterization of the postembryonic development of *P. marginemaculatus* is available in the works of Weygoldt (Weygoldt, 1969; 1970). The following summary is after Weygoldt

(1975), complemented with observations from the present study. We note that the timing of embryonic stages is approximate, as the temperature in Weygoldt (1975) was kept in a range of 24–27˚C.

In our colony, a sample of 18 clutches from different females had an average of 19 eggs (min: 8 eggs; max: 39 eggs). Each egg is ovoid and measures 1.2–1.4 mm at the longest diameter. The yolk granules are light green, and fixation turns them light yellow. Upon secreting the brood sac and eggs into the ventral side of the opisthosoma, the brood sac is transparent, but gradually hardens and becomes dark brown in the course of two days. Around 6 dAEL, a blastoderm is formed. At 7–8 dAEL, the yolk is more condensed, a perivitelline space is formed, cells move into the yolk presumably in the region of the future blastopore. At 8–9 dAEL a blastopore is recognizable on the dorsal surface of the embryo, and a germ disc is formed. Towards 10 dAEL, the germ band starts to take form, the blastopore region is displaced posteriorly, and the first signs of segmentation of the prosoma are visible. A presumable cumulus, a group of migrating cells with dorso-ventral organizing properties, was reported by Weylgodt (1975) at this stage, but was not investigated by us. At 11-12 dAEL, the nascent prosomal segments elongate anteriorly and by 13-14 dAEL the segmented germ band occupies the ventral hemisphere of the egg. The limb buds of prosomal appendages begin to appear (Fig. 2A). The process of reversion begins, with a sagittal split of the germ band (Fig. 2A). From this point, until 19 dAEL, the ventral sulcus progressively enlarges with the dorsal displacement of both halves, and then begin to ventrally fuse again starting anteriorly (Fig. 2A–E). The head lobes on 15 dAEL are wing-shaped and uniform (Fig. 2 F). From 15–19 dAEL, ectodermal cells invaginate in the ventral midline and head lobes (neural precursor cells), which can be seen as evenly spaced dark dots (Fig. 2 F–H). Concomitantly, the anterior rim of the head lobes forms semi lunar groves (folds over itself) (Fig. 2 F–H). Opisthosomal segments 1–12 sequentially appear from the posterior growth zone (Fig. I–K). At 19 dAEL, the yolk moves into the caudal papilla (growth zone) and opisthosoma flexes ventrally (Fig. 2 K, N). The first pair of legs (future antenniform legs) is longer than the other appendages already on an early limb bud stage (15 dAEL), and more clearly on subsequent stages (Fig. L–N). A protuberance on the proximal end of the second walking leg pair (L2), the nascent lateral organ (osmoregulatory embryonic organ), is discernible at 16 dAEL and later stages, and becomes reniform (Fig. L–N). From 20–21 dAEL, the embryo begins to secrete a cuticle, which is darker on the fully formed lateral organ. The head lobes have completely folded onto themselves, and the distal segment of the chelicera is sclerotized. The embryo hatches into a deutembryo stage while still inside the

brood sac (Fig. 1 F–H). Deutembryos remain in the brood sac for further 70 days without discernible external changes. The primordia of the eyes are formed towards the end of deutembryo development (70–106 dAEL), and eye spots of the median and lateral eyes become visible. From 90-106 dAEL the deutembryos molt into praenymphs, leave the brood sac and climb to their mom's back. For a histological description of gastrulation, of the mesoderm, brain and nervous system, digestive system and gonad formation, we refer the reader to the exquisite original descriptions of Weygoldt (1975).

Phrynus marginemaculatus embryonic transcriptome

In order to provide a comprehensive resource for Amblypygi to facilitate developmental genetic study and comparative genomics, we assembled an embryonic transcriptome spanning different embryonic stages. The assembly of *P. marginemaculatus* transcriptome resulted in 544.372 transcripts composed of 277.432.101 bp and N50 of 440 bp. BUSCO scores, which reports the presence and number of copies of widely conserved single-copy genes (n=1066), indicated 94.2% completeness with 5.9% of genes duplicated. From the total number of transcripts (including isoforms), we predicted 37.540 peptide sequences with the Trinotate pipeline with a top blastp hit in Swiss-Prot database. A total of 801 of these peptides (2.1%) had a top hit to non-metazoan proteins, and presumed microbial contaminants.

To investigate the possibility of systemic gene duplication in Amblypygi and further test the transcriptome completeness, we searched for all ten Hox genes, emphasizing discovery of paralogs known from in the genomes of the spider *Parasteatoda tepidariorum* (except for *fushi tarazu*) and the scorpion *Centruroides sculpturatus* (except for *Hox3*) (Leite et al., 2018; Schwager et al., 2017; Sharma, Schwager, Extavour, & Wheeler, 2014b). One of the *Hox3* copies of *P. tepidariorum* has no discernible expression pattern (Schwager et al., 2017) and had an unusually long branch in our analysis (Fig. S1). We therefore removed this copy from our analysis given its questionable annotation. We found orthologs of all ten Hox genes in *Phrynus marginemcaulatus*, namely *labial*, *proboscipedia*, *Hox3*, *Deformed*, *Sex combs reduced*, *fushi tarazu*, *Antennapedia*, *Ultrabithorax*, *abdominal A* and *Abdominal B* (Fig. 3A–B). We found evidence that all Hox genes, except *proboscipedia* are assembled in two Trinity genes and have amino acid differences (Fig. 3B). A *Pmar-Dfd* and *Pmar-abdA* were also found in a third Trinity gene, but their non-overlapping position on the alignment and nearly identic amino acid sequence to the respective paralog 2 indicate that they are

fragmented assemblies of the same copy. These results suggest that Amblypygi share a duplicated Hox cluster with 19 Hox genes with spiders and scorpions, and that these copies are transcriptionally active during embryogenesis.

Gene expression analyses in *Phrynus marginemaculatus*

All three methods used here for fixing embryos of *P. marginemaculatus* yield embryos which are suitable for in situ hybridization (ISH). However, fixation of intact embryos in formaldehyde/heptane phase sometimes results in the vitelline membrane adhering to the embryos. Upon dissection of the vitelline membrane for ISH, parts of the embryo are commonly lost. Piercing a hole in the embryo for fixation in formaldehyde achieves a similar result, and is therefore not recommended. Dissecting vitelline membrane under PBS and immediately fixing the embryos in formaldehyde yielded the best results. We did not detect any difference in the signal-to-background ratio of colorimetric ISH between embryos fixed for 2 h or 24 h. To test gene expression assays and investigate the genetic patterning of antenniform legs, we selected the leg gap genes *Distal-less*, *dachshund* and *homothorax*, which constitute the subset of PD axis patterning genes associated with functional datasets in other arachnid model species (Schoppmeier & Damen, 2001; Sharma et al., 2013; 2015b).

Distal-less identification and expression

Similar to other arachnopulmonates and arthropods in general, a single *Distal-less* gene, *Pmar-Dll*, was found by similarity searches and its orthology to other metazoan *Distal-less* genes was confirmed with phylogenetic analysis (Fig. S2). *Pmar-Dll* is strongly expressed in all developing appendages, from early limb bud stage (15 dAEL) and is localized to the distal portion of the chelicera, pedipalp and legs throughout leg elongation (Fig. 4 A–I; Fig. 5A–L). In 17-18 dAEL embryos, the expression is heterogeneous and forms bands of stronger expression on the forming podomeres of the pedipalps and legs (Fig. 5 H–L). We did not detect expression on ventral midline (*contra* Sharma et al. 2012 and Mittmann and Scholtz 2001), or in the opisthosoma, and observed only diffuse expression on the head lobes of the stages surveyed. Expression on L1 of 16-17 dAEL embryos is subtly stronger on the proximal part of the expression domain (Fig. 5C–C'), but we did not detect clear differences in younger or older embryonic stages. The proximal and distal boundaries of strong *Distal-*

less expression do not differ between L1 and the other legs, spanning two-thirds of the legs from the tip of the tarsus and excluding the most proximal third (Fig. 5C, 5I).

In contrast to other arachnid embryos (mygalomorph spiders (Pechmann & Prpic, 2009); araneomorph spiders (Prpic & Damen, 2004; Schoppmeier & Damen, 2001); Opiliones, Sharma et al. 2012; and mites (Barnett & Thomas, 2013b; Thomas & Telford, 1999)), *Dll* expression was not detected as a strong domain in the endite of pedipalp, which is very inconspicuous at these embryonic stages. We were not able to assess *Dll* expression in the pedipalpal endite in deutembryo stages due to deposition of cuticle.

dachshund identification and expression

dachshund is present as a single copy in Arthropoda, but is found independently duplicated in Arachnopulmonata and Xiphosura (Nolan et al., 2020; Turetzek et al., 2015). We found two Trinity genes with high similarity to *Dmel-dac* and confirmed their identity as dachshund paralogs with a phylogenetic analysis (Fig. S3). *Pmar-dac1* and *Pmar-dac2* are each nested in a clade with paralogs 1 and 2 of other arachnopulmonates, which appears as independent from horseshoe crab duplications (Fig. S3).

Pmar-dac1 is strongly expressed as broad mid band in the pedipalp and four pairs of legs (Fig. 6 A–F). This sharp mid band excludes the most proximal and the distal domains of these appendages (Fig. 7). No staining was detected on the chelicera (Fig. 6 A–F; 7 A, E). Additionally, expression occurs in three domains in the head lobes and strongly on the ventral midline of the prosoma. The continuous expression on the ventral midline stops before the opisthosoma (Fig. 6 A–F).

Pmar-dac2 is expressed as ring at the proximal region of chelicera, pedipalp and legs (Fig. 6 G–I). On 16-17 dAEL embryo a second thinner ring of expression is also present on the pedipalps and legs (Fig. 6 G–I; 7 I–L). Expression domains also occur on the neuromere of L1 and pedipalp, being larger on the pedipalp neuromere (Fig. 6 G). Three spot domains also occur on O1, O2 and O3 segments (Fig. 6 H–I).

homothorax identification and expression

Similar to the case with arachnid *dachshund*, *homothorax* is also found duplicated in arachnopulmonates (Leite et al., 2018; Turetzek et al., 2017). We annotated two Trinity genes in *P. marginemaculatus* transcriptome and the phylogenetic analysis shows that each copy is nested in two clades with the arachnopulmonate paralogs (Fig. S4).

Pmar-hth1 is conspicuously expressed on the developing appendages throughout the stages studied (15-18 dAEL; Fig. 8–9). On 16-17 dAEL embryos, *Pmar-hth1* is expressed more strongly on the proximal parts of the chelicera, pedipalp, and legs, and is absent in a small distal domain (Fig. 9 A–D). On 17-18 dAEL, expression in all elongated appendages is similar, and spans most of the appendage length except for a small distal territory (Fig. 9 E-H). Additionally, three stronger stripe domains occur distal to the coxa of pedipalp and legs. Expression in L1 and other legs is similar in the studied stages, save for a slightly expanded distal domain on the proximal tarsus of L1 (Fig. 9 G–H). Expression on the ventral ectoderm and head lobes is weak and homogenous in early stages, and becomes stronger in 17-18 dAEL (not shown)

Pmar-hth2 is expressed in the developing appendages, but is reduced in intensity and different in pattern in comparison to *Pmar-hth1* (Fig. 8 B–B'). *Pmar-hth2* spans the whole chelicera (Fig. 9 I). Expression on the pedipalp spans most of the appendage, excluding only a distal territory (Fig. 9 J). In addition, there is a proximal and a sub terminal strong domain (Fig. 9 J). Expression on L1 and other legs is identical in all stages studies. *Pmar-hth2* expression on the legs is consistently weaker in comparison to the pedipalp, but likewise possess a proximal and a distal sub-terminal domain (Fig. 9K–L). Expression on the ventral ectoderm, opisthosoma and head lobes is ubiquitous (Fig. 8B).

Discussion

Whip spiders retain arachnopulmonate gene duplications

Changes in Hox gene expression, regulation and targets are linked to changes in morphology, and Hox gene duplications have also been implicated in morphological innovations (Hughes & Kaufman, 2002; C. L. H. A. T. C. Kaufman, 2000; Ronshaugen, McGinnis, & McGinnis, 2002; Wagner, Amemiya, & Ruddle, 2003). Duplication in the Hox cluster is common in the vertebrates, which may have up to eight Hox clusters (teleost fishes)

due to successive rounds of genome duplications (Wagner et al., 2003). On the other hand, genome and Hox cluster duplication is considered rare in Arthropoda (Pace, Grbić, & Nagy, 2016). Complete Hox cluster duplication in the phylum has only been reported in horseshoe crabs (Xiphosura) (Kenny et al., 2015; Nossa et al., 2014; Shingate et al., 2020; Zhou et al., 2020), and in spiders and scorpions (presumed ancestral in Arachnopulmonata). The phylogenetic placement of Amblypygi makes this group an opportune system to test the downstream prediction that *P. marginemaculatus* retains and expresses Hox paralogs shared by spiders and scorpions. In accordance with this hypothesis, we discovered that the whip spider *P. marginemaculatus* presents homologs of all ten Hox genes, and all excepting *proboscipedia* appear to be duplicated, as supported by our alignment and phylogenetic analysis.

A second line of evidence of a shared genome duplication event comes from conserved expression patterns of leg gap gene paralogs. It has recently been shown that duplicates of leg patterning genes *extradenticle*, *optomotor blind*, *dachshund* (*dac*) and *homothorax* (*hth*) present one copy with the arthropod plesiomorphic expression domain, and a second copy with a divergent expression shared between a spider and a scorpion (Nolan et al., 2020). For instance, *dac1* of surveyed arachnopulmonates retains the plesiomorphic expression pattern of a broad mid band in the appendages, the condition observed in the single copy *dac* of all non-arachnopulmonate arachnids surveyed to date (Barnett & Thomas, 2013b; Sharma, Schwager, Extavour, & Giribet, 2012a), whereas *dac2* is expressed as a proximal and a mid domain (Nolan et al., 2020; Pechmann & Prpic, 2009; Prpic & Damen, 2004; Turetzek et al., 2015). The same is true for *homothorax*: *hth1* retains a plesiomorphic expression pattern on the proximal-mid appendage excluding the tarsus, whereas *hth2* presents a strong short proximal domain and weakly striped pattern distally (Nolan et al., 2020; Pechmann & Prpic, 2009; Prpic & Damen, 2004; Turetzek et al., 2017). In the whip spider *P. marginemaculatus*, we indeed recovered two copies of *dachshund* and *homothorax*, with paralogs nested in two clades of arachnopulmonate copies with high nodal support (Fig. S3, S4). Moreover, *Pmar-dac* and *Pmar-hth* copies share with spider and scorpion the same pattern of expression of their paralogs: *Pmar-dac1/2* and *Pmar-hth1/2* conserve the plesiomorphic expression pattern of arachnids, while the copy 2 retain the arachnopulmonate-specific pattern. These data, together with the evidence from Hox gene duplications and the topologies of the *dac* and *hth* gene trees, provide compelling support for genome duplication as a synapomorphy of Arachnopulmonata.

A *dachshund2* domain in the two-segmented clasp-knife chelicera of *P. marginemaculatus*

Expression of *Pmar-Dll*, *Pmar-dac1/2* and *Pmar-hth1/2* on the appendages is largely similar to spiders and scorpions (see above) (Nolan et al., 2020; Pechmann & Prpic, 2009; Prpic et al., n.d.; Prpic & Damen, 2004; Turetzek et al., 2015; 2017). A notable difference in the chelicera of the whip spider is the retention of proximal expression of one of the *dachshund* paralogs. In arachnids with three segmented chelicerae, such as daddy-long-legs, *dac* is expressed in the proximal segment of the appendage (Sharma, Schwager, Extavour, & Giribet, 2012a). The same is true for the three-segmented chelicera of scorpions, in which both *dac1* and *dac2* are expressed in the proximal segment (Nolan et al., 2020). In the two-segmented chelicera of spiders, *dac1* is not expressed in the chelicera save for a non-ectodermal faint staining in late embryonic stage (Abzhanov & Kaufman, 2000; Pechmann & Prpic, 2009; Prpic et al., n.d.; Prpic & Damen, 2004; Turetzek et al., 2015). *dac2* of spiders is also largely not expressed in the chelicera, save for small ventral domain at the base of the chelicera of *Parasteatoda tepidariorum* and *Pholcus phalangioides* (Turetzek et al., 2015). It has been proposed that the loss of a proximal *dac* domain is associated with the loss of the proximal segment in the chelicera of spider and other arachnids. This hypothesis is supported by functional data in the daddy-long-leg *P. opilio*: knockdown of the single-copy *dac* resulted in the loss of the proximal segment of the chelicera (as well as mid-segment truncations in pedipalps and legs) (Sharma et al., 2013). Similar to spiders, the two-segmented chelicera of the whip spider *P. marginemaculatus* does not express *Pmar-dac1*. Nonetheless, a clear complete ring of proximal expression was detected for *Pmar-dac2*.

In contrast to the classic leg gap phenotype incurred by knockdown of the ancestral *dac* copy in the harvestman, knockdown of *dac2* in the spider *P. tepidari*orum resulted in the loss of the patella-tibia segment boundary in the pedipalp and walking legs; effects of this knockdown on the chelicera were not reported by the authors, nor is the function of *dac1* known in *P. tepidariorum* (Turetzek et al. 2015). Given the interpretation that *dac2* has a derived role in patterning a segment boundary in the spider, the incidence of the *Pmar-dac2* stripe in the middle of the whip spider chelicera (and the absence of *Pmar-dac1* in the chelicera) is tentatively hypothesized here to constitute evidence of a segment boundary patterning activity that separates the basal and distal cheliceral segment of Amblypygi (rather than evidence of a proximal segment identity in whip spiders that is homologous to the proximal cheliceral segment of groups like harvestmen and scorpions). Exploring this

hypothesis in future will require the establishment of RNAinterference tools in *P. marginemaculatus.*

Antenniform leg distal allometry is specified early in development

To investigate a possible role of changes in leg gap genes expression in the patterning of the antenniform leg pair (L1) of whip spiders, we specifically searched for changes in expression domain between embryonic antenniform leg (L1) and the posterior legs (L2–4). The expression patterns of *Pmar-Dll*, *Pmar-dac1/2* and *Pmar-hth1/2* are mostly identical between the antenniform leg L1 and the posterior legs. We found only a slightly expanded *Pmar-hth1* domain in the distal leg (compare Fig. G–H). It is unclear if this difference bears any functional significance in the differential fate of L1. Similar distal expression dynamics appear to distinguish the identity of the pedipalp and walking legs of the harvestman, as knockdown of the single copy of *hth* in *P. opilio* results in homeotic transformation of pedipalps to legs (Sharma et al., 2015b).

Besides the difference in sensory equipment, the antenniform leg pair of adults differ from the posterior walking legs in being much longer, and presenting numerous articles (pseudo-segments) on the tibia, metatarsus and especially the tarsus, whereas the walking legs have pseudo-segments only in the tarsus (Igelmund, 1987; Santer & Hebets, 2011; Weygoldt, 2000). Antenniform legs may be more than 2.5 times longer than the walking legs, and this allometry in adults is mostly accounted for by the length added by the distal leg segments, which may attain more than 100 distal articles (tibiomeres + tarsomeres) (Igelmund, 1987). Understanding the timing of the ontogenetic divergence of L1 relative to the walking legs is crucial for circumscribing target stages for investigation of the genetic patterning of this phenomenon. Current evidence indicates that this allometry on the antenniform legs takes place both embryonically and post embryonically.

The preaenymph, the stage that molts from the deutembryo and climbs to the mother's back, has the full number of tibiomeres, but not of tarsomeres. The final number of tarsomeres is added in the next molt to the protonymph (Beck, Foelix, Gödeke, & Kaiser, 1977; Igelmund, 1987), and from this moment onwards the subsequent growth is isometric (Beck et al., 1977; Igelmund, 1987). In embryos of *P. marginemaculatus*, Weygoldt (1975) observed that the primordia of L1 are the first to appear in the germ band and are already longer than the

remaining prosomal appendages, an observation paralleling the allometric growth of the L2 limb bud of the harvestman *P. opilio* (wherein L2 is the longest leg and also bears the most tarsomeres) (Sharma, Schwager, Extavour, & Giribet, 2012b). It is presently unclear at what point in development the distal podemeres of antenniform legs attain their allometry with respect to the proximal podomeres in the whip spider. In other words, are embryonic legs simply growing longer overall with respect to walking legs, or are they longer due to distal growth? The expression pattern *dachshund* in *P. marginemaculatus* early embryos reveals a further interesting aspect of this allometry. The expression of *dac* (including duplicates) in the legs of arachnids surveyed to date occurs on podomeres proximal to tibia, so that the tibia-metatarsus-tarsus territory may be identified as the a *dac*-free domain (Abzhanov & Kaufman, 2000; Barnett & Thomas, 2013b; Nolan et al., 2020; Pechmann & Prpic, 2009; Prpic & Damen, 2004; Sharma et al., 2013; Turetzek et al., 2015). The distal boundary of *Pmar-dac1* an *Pmar-dac2* in stages long before podomere formation reveals that the distal domain (*Pmar-dac1* free cells) of L1 is already longer with respect to the proximal leg and the other legs (compare Fig. 7 C, D). These data support the inference that the distal allometry, and by extension the antenniform leg fate, are already specified from the onset of limb bud development.

Conclusion

The study of the embryology of Amblypygi has faced 45 years of hiatus since the seminal work describing the development of *Phrynus marginemaculatus* (Weygoldt, 1975). Here, we take the first steps in establishing *P. marginemaculatus* as a model for modern chelicerate evolutionary developmental study and for comparative genomics, with emphasis on discovering the genetic specification of the eponymous sensory legs. Future efforts to uncover the genetic underpinnings of this fascinating convergence with the mandibulate antenna should prioritize discovery of leg fate specification mechanisms in early whip spider development. Despite the establishment of a few promising arachnid models for studying chelicerate embryology, a pervasive challenge has been the establishment of toolkits for testing gene function (Akiyama-Oda & Oda, 2003; Khila & Grbić, 2007b; Schoppmeier & Damen, 2001; Sharma et al., 2013). Therefore, future efforts to study whip spider development must emphasize the development of functional for functional experiments in *P. marginemaculatus*.

Acknowledgments

This work is dedicated to Peter Weygoldt, whose pioneer work in the development of *Phrynus marginemaculatus* and contributions to the study of Amblypygi biology continue to inspire the authors of this paper. Sequencing was performed at the University of Wisconsin-Madison BioTechnology Center. Microscopy was performed at the Newcomb Imaging Center, Department of Botany, University of Wisconsin-Madison. GG was supported by a Wisconsin Alumni Research Foundation Fall Research Competition award. Materials for study were supported by an Oscar Franke student competition award to GG from the International Society of Arachnology. This material is based on work supported by the National Science Foundation under grant IOS-1552610 to PPS.

References

Abzhanov, A., & Kaufman, T. C. (2000). Homologs of Drosophila Appendage Genes in the Patterning of Arthropod Limbs. *Developmental Biology*, *227*(2), 673–689. http://doi.org/10.1006/dbio.2000.9904

Akiyama-Oda, Y., & Oda, H. (2003). Early patterning of the spider embryo: a cluster of mesenchymal cells at the cumulus produces Dpp signals received by germ disc epithelial cells. *Development*, *130*(9), 1735–1747. http://doi.org/10.1242/dev.00390

Akiyama-Oda, Y., & Oda, H. (2006). Axis specification in the spider embryo: *dpp* is required for radial-to-axial symmetry transformation and *sog* for ventral patterning. *Development*, *133*(12), 2347–2357. http://doi.org/10.1242/dev.02400

Akiyama-Oda, Y., & Oda, H. (2010). Cell migration that orients the dorsoventral axis is coordinated with anteroposterior patterning mediated by Hedgehog signaling in the early spider embryo. *Development*, *137*(8), 1263–1273. http://doi.org/10.1242/dev.045625

Ballesteros, J. A., & Sharma, P. P. (2019). A Critical Appraisal of the Placement of Xiphosura (Chelicerata) with Account of Known Sources of Phylogenetic Error. *Systematic Biology*, *33*, 440–22. http://doi.org/10.1093/sysbio/syz011

Barnett, A. A., & Thomas, R. H. (2012). The delineation of the fourth walking leg segment is temporally linked to posterior segmentation in the mite *Archegozetes longisetosus* (Acari: Oribatida, Trhypochthoniidae). *Evolution & Development*, *14*(4), 383–392. http://doi.org/10.1111/j.1525-142X.2012.00556.x

Barnett, A. A., & Thomas, R. H. (2013a). Posterior Hox gene reduction in an arthropod: *Ultrabithorax* and *Abdominal-B* are expressed in a single segment in the mite *Archegozetes longisetosus*. *EvoDevo*, *4*(1), 23. http://doi.org/10.1186/2041-9139-4-23

Barnett, A. A., & Thomas, R. H. (2013b). The expression of limb gap genes in the mite *Archegozetes longisetosus* reveals differential patterning mechanisms in chelicerates. *Evolution & Development*, *15*(4), 280–292. http://doi.org/10.1111/ede.12038

Beck, L., Foelix, R., Gödeke, E., & Kaiser, R. (1977). Morphology, larval development, and hair sensilla of the antenniform legs of the whip spider *Heterophrynus longicornis* Butler (Arach., Amblypygi). *Zoomorphologie*, *88*(3), 259–276. http://doi.org/10.1007/BF00995476

Blackburn, D. C., Conley, K. W., Plachetzki, D. C., Kempler, K., Battelle, B.-A., & Brown, N. L. (2008). Isolation and expression of Pax6and atonalhomologues in the American

horseshoe crab, Limulus polyphemus. *Developmental Dynamics*, *237*(8), 2209–2219. http://doi.org/10.1002/dvdy.21634
Bolger, A. M., Lohse, M., & Usadel, B. (2014). Trimmomatic: a flexible trimmer for Illumina sequence data. *Bioinformatics*, *30*(15), 2114–2120. http://doi.org/10.1093/bioinformatics/btu170
Bryant, D. M., Johnson, K., DiTommaso, T., Tickle, T., Couger, M. B., Payzin-Dogru, D., et al. (2017). A Tissue-Mapped Axolotl De Novo Transcriptome Enables Identification of Limb Regeneration Factors. *CellReports*, *18*(3), 762–776. http://doi.org/10.1016/j.celrep.2016.12.063
Casares, F., & Mann, R. S. (1998). Control of antennal versus leg development in *Drosophila*. *Nature*, *392*(6677), 723–726. http://doi.org/10.1038/33706
Chapin, K. J., & Hebets, E. A. (2016). The behavioral ecology of amblypygids. *Journal of Arachnology*, *44*(1), 1–14. http://doi.org/10.1636/V15-62.1
Chipman, A. D., Ferrier, D. E. K., Brena, C., Qu, J., Hughes, D. S. T., Schröder, R., et al. (2014). The First Myriapod Genome Sequence Reveals Conservative Arthropod Gene Content and Genome Organisation in the Centipede Strigamia maritima. *PLoS Biology*, *12*(11), e1002005–24. http://doi.org/10.1371/journal.pbio.1002005
Damen, W. G. M., Hausdorf, M., Seyfarth, E.-A., & Tautz, D. (1998). A conserved mode of head segmentation in arthropods revealed by the expression pattern of Hox genes in a spider. *Proceedings of the National Academy of Sciences*, *95*(18), 10665–10670. http://doi.org/10.1038/376165a0
Dearden, P. K. (2002). Expression of pair-rule gene homologues in a chelicerate: early patterning of the two-spotted spider mite *Tetranychus urticae*. *Development*, *129*(23), 5461–5472. http://doi.org/10.1242/dev.00099
Dong, P. D. S., Dicks, J. S., & Panganiban, G. (2002). Distal-less and homothorax regulate multiple targets to pattern the Drosophila antenna. *Development*, *129*(8), 1967–1974.
Dong, P. D., Chu, J., & Panganiban, G. (2001). Proximodistal domain specification and interactions in developing Drosophila appendages. *Development*, *128*(12), 2365–2372. http://doi.org/10.3390/jdb6030017
Duncan, D. M., Burgess, E. A., & Duncan, I. (1998). Control of distal antennal identity and tarsal development in Drosophila by spineless-aristapedia, a homolog of the mammalian dioxin receptor. *Genes & Development*, *12*(9), 1290–1303. http://doi.org/10.1101/gad.12.9.1290
Fowler-Finn, K. D., & Hebets, E. A. (2006). An Examination of agonistic interactions in the whip spider *Phrynus marginemaculatus* (Arachnida, Amblypygi). *Journal of Arachnology*, *34*(1), 62–76. http://doi.org/10.1636/S04-104.1
Gainett, G., Ballesteros, J. A., Kanzler, C. R., Zehms, J. T., Zern, J. M., Aharon, S., et al. (2020). How spiders make their eyes: Systemic paralogy and function of retinal determination network homologs in arachnids. *bioRxiv*, *129*(5), 1143–34. http://doi.org/10.1101/2020.04.28.067199
Giribet, G. (2018). Current views on chelicerate phylogeny—A tribute to Peter Weygoldt. *Zoologischer Anzeiger - a Journal of Comparative Zoology*, *273*, 7–13. http://doi.org/10.1016/j.jcz.2018.01.004
Gouy, M., Guindon, S., & Gascuel, O. (2010). SeaView Version 4: A Multiplatform Graphical User Interface for Sequence Alignment and Phylogenetic Tree Building. *Molecular Biology and Evolution*, *27*(2), 221–224. http://doi.org/10.1093/molbev/msp259
Grabherr, M. G., Haas, B. J., Yassour, M., Levin, J. Z., Thompson, D. A., Amit, I., et al. (2011). Full-length transcriptome assembly from RNA-Seq data without a reference genome. *Nature Biotechnology*, *29*(7), 644–652. http://doi.org/10.1038/nbt.1883

Grbić, M., Khila, A., Lee, K.-Z., Bjelica, A., Grbić, V., Whistlecraft, J., et al. (2007). Mity model: *Tetranychus urticae*, a candidate for chelicerate model organism. *BioEssays*, *29*(5), 489–496. http://doi.org/10.1002/bies.20564

Grbić, M., Van Leeuwen, T., Clark, R. M., Rombauts, S., Rouzé, P., Grbić, V., et al. (2011). The genome of *Tetranychus urticae* reveals herbivorous pest adaptations. *Nature*, *479*(7374), 487–492. http://doi.org/10.1038/nature10640

Gulia-Nuss, M., Nuss, A. B., Meyer, J. M., Sonenshine, D. E., Roe, R. M., Waterhouse, R. M., et al. (2016). Genomic insights into the *Ixodes scapularis* tick vector of Lyme disease. *Nature Communications*, *7*(1), 10507–13. http://doi.org/10.1038/ncomms10507

Harvey, M. S. (2013). ***Whip spiders of the World, version 1.0***. Perth: Western Australian Museum. Retrieved from http://www.museum.wa.gov.au/catalogues/whip-spiders

Herndon, N., Shelton, J., Gerischer, L., Ioannidis, P., Ninova, M., Dönitz, J., et al. (2020). Enhanced genome assembly and a new official gene set for Tribolium castaneum, 1–13. http://doi.org/10.1186/s12864-019-6394-6

Hughes, C. L., & Kaufman, T. C. (2002). Hox genes and the evolution of the arthropod body plan. *Evolution & Development*, *4*(6), 459–499.

Igelmund, P. (1987). Morphology, sense organs, and regeneration of the forelegs (whips) of the whip spider *Heterophrynus elaphus* (Arachnida, Amblypygi). *Journal of Morphology*, *193*(1), 75–89. http://doi.org/10.1002/jmor.1051930108

Kaufman, C. L. H. A. T. C. (2000). RNAi analysis of *Deformed*, *proboscipedia* and *Sex combs reduced* in the milkweed bug *Oncopeltus fasciatus*: novel roles for Hox genes in the Hemipteran head, 1–12.

Kenny, N. J., Chan, K. W., Nong, W., Qu, Z., Maeso, I., Yip, H. Y., et al. (2015). Ancestral whole-genome duplication in the marine chelicerate horseshoe crabs. *Heredity*, *116*(2), 190–199. http://doi.org/10.1038/hdy.2015.89

Khadjeh, S., Turetzek, N., Pechmann, M., Schwager, E. E., Wimmer, E. A., Damen, W. G. M., & Prpic, N. M. (2012). Divergent role of the Hox gene *Antennapedia* in spiders is responsible for the convergent evolution of abdominal limb repression. *Proceedings of the National Academy of Sciences*, *109*(13), 4921–4926. http://doi.org/10.1073/pnas.1116421109

Khila, A., & Grbić, M. (2007a). Gene silencing in the spider mite Tetranychus urticae: dsRNA and siRNA parental silencing of the Distal-less gene, *217*(3), 241–251. http://doi.org/10.1007/s00427-007-0132-9

Khila, A., & Grbić, M. (2007b). Gene silencing in the spider mite Tetranychus urticae: dsRNA and siRNA parental silencing of the Distal-less gene. *Development Genes and Evolution*, *217*(3), 241–251. http://doi.org/10.1007/s00427-007-0132-9

Koressaar, T., & Remm, M. (2007). Enhancements and modifications of primer design program Primer3. *Bioinformatics*, *23*(10), 1289–1291. http://doi.org/10.1093/bioinformatics/btm091

Leite, D. J., Baudouin-Gonzalez, L., Iwasaki-Yokozawa, S., Lozano-Fernandez, J., Turetzek, N., Akiyama-Oda, Y., et al. (2018). Homeobox Gene Duplication and Divergence in Arachnids. *Molecular Biology and Evolution*, *35*(9), 2240–2253. http://doi.org/10.1093/molbev/msy125

Lozano-Fernandez, J., Tanner, A. R., Giacomelli, M., Carton, R., Vinther, J., Edgecombe, G. D., & Pisani, D. (2019). Increasing species sampling in chelicerate genomic-scale datasets provides support for monophyly of Acari and Arachnida. *Nature Communications*, 1–8. http://doi.org/10.1038/s41467-019-10244-7

Mittmann, B., & Scholtz, G. (2001). *Distal-less* expression in embryos of *Limulus polyphemus* (Chelicerata, Xiphosura) and *Lepisma saccharina* (Insecta, Zygentoma) suggests a role in the development of mechanoreceptors, chemoreceptors, and the CNS.

Development Genes and Evolution, *211*(5), 232–243. http://doi.org/10.1007/s004270100150

Nguyen, L.-T., Schmidt, H. A., Haeseler, von, A., & Minh, B. Q. (2015). IQ-TREE: a fast and effective stochastic algorithm for estimating maximum-likelihood phylogenies. *Molecular Biology and Evolution*, *32*(1), 268–274. http://doi.org/10.1093/molbev/msu300

Nolan, E. D., Santibáñez López, C. E., & Sharma, P. P. (2020). Developmental gene expression as a phylogenetic data class: support for the monophyly of Arachnopulmonata. *Development Genes and Evolution*, *230*(2), 137–153. http://doi.org/10.1007/s00427-019-00644-6

Nossa, C. W., Havlak, P., Yue, J.-X., Lv, J., Vincent, K. Y., Brockmann, H. J., & Putnam, N. H. (2014). Joint assembly and genetic mapping of the Atlantic horseshoe crab genome reveals ancient whole genome duplication. *GigaScience*, *3*(1), 708–21. http://doi.org/10.1186/2047-217X-3-9

Oda, H., & Akiyama-Oda, Y. (2008). Differing strategies for forming the arthropod body plan: lessons from Dpp, Sog and Delta in the fly *Drosophila* and spider *Achaearanea*. *Development, Growth & Differentiation*, *50*(4), 203–214. http://doi.org/10.1111/j.1440-169X.2008.00998.x

Pace, R. M., Grbić, M., & Nagy, L. M. (2016). Composition and genomic organization of arthropod Hox clusters. *EvoDevo*, *7*(1), 11–11. http://doi.org/10.1186/s13227-016-0048-4

Paese, C. L. B., Schoenauer, A., Leite, D. J., Russell, S., & McGregor, A. P. (2018). A SoxB gene acts as an anterior gap gene and regulates posterior segment addition in a spider. *eLife*, *7*, 1735. http://doi.org/10.7554/eLife.37567

Pechmann, M., & Prpic, N.-M. (2009). Appendage patterning in the South American bird spider Acanthoscurria geniculata (Araneae: Mygalomorphae). *Development Genes and Evolution*, *219*(4), 189–198. http://doi.org/10.1007/s00427-009-0279-7

Pechmann, M., Benton, M. A., Kenny, N. J., Posnien, N., & Roth, S. (2017). A novel role for *Ets4* in axis specification and cell migration in the spider *Parasteatoda tepidariorum*. *eLife*, *6*. http://doi.org/10.7554/eLife.27590

Pechmann, M., Khadjeh, S., Turetzek, N., McGregor, A. P., Damen, W. G. M., & Prpic, N.-M. (2011). Novel function of *Distal-less* as a gap gene during spider segmentation. *PLoS Genetics*, *7*(10), e1002342. http://doi.org/10.1371/journal.pgen.1002342

Pechmann, M., Schwager, E. E., Turetzek, N., & Prpic, N.-M. (2015). Regressive evolution of the arthropod tritocerebral segment linked to functional divergence of the Hox gene *labial*. *Proceedings of the Royal Society B: Biological Sciences*, *282*(1814), 20151162–6. http://doi.org/10.1098/rspb.2015.1162

Prpic, N. M., Janssen, R., Wigand, B., Developmental, M. K., 2003. (n.d.). Gene expression in spider appendages reveals reversal of exd/hth spatial specificity, altered leg gap gene dynamics, and suggests divergent distal …. *Elsevier*
. http://doi.org/10.1016/S0012-1606(03)00466-4

Prpic, N.-M., & Damen, W. M. (2004). Expression patterns of leg genes in the mouthparts of the spider Cupiennius salei (Chelicerata: Arachnida). *Development Genes and Evolution*, *214*(6), 1–7. http://doi.org/10.1007/s00427-004-0393-5

Rayor, L. S., & Taylor, L. A. (2006). SOCIAL BEHAVIOR IN AMBLYPYGIDS, AND A REASSESSMENT OF ARACHNID SOCIAL PATTERNS. *Journal of Arachnology*, *34*(2), 399–421. http://doi.org/10.1636/S04-23.1

Ronshaugen, M., McGinnis, N., & McGinnis, W. (2002). Hox protein mutation and macroevolution of the insect body plan. *Nature*, *415*(6874), 914–917. http://doi.org/10.1038/nature716

Samadi, L., Schmid, A., & Eriksson, B. J. (2015). Differential expression of retinal determination genes in the principal and secondary eyes of *Cupiennius salei* Keyserling (1877). *EvoDevo*, *6*(1), 16–17. http://doi.org/10.1186/s13227-015-0010-x

Santer, R. D., & Hebets, E. A. (2009). Tactile learning by a whip spider, *Phrynus marginemaculatus* C.L. Koch (Arachnida, Amblypygi). *Journal of Comparative Physiology A*, *195*(4), 393–399. http://doi.org/10.1007/s00359-009-0417-8

Santer, R. D., & Hebets, E. A. (2011). The Sensory and Behavioural Biology of Whip Spiders (Arachnida, Amblypygi). *Spider Physiology and Behaviour* (1st ed., Vol. 41, pp. 1–64). Elsevier Ltd. http://doi.org/10.1016/B978-0-12-415919-8.00001-X

Santos, V. T., Ribeiro, L., Fraga, A., de Barros, C. M., Campos, E., Moraes, J., et al. (2013). The embryogenesis of the Tick *Rhipicephalus* (*Boophilus*) *microplus*: The establishment of a new chelicerate model system. *Genesis*, *51*(12), 803–818. http://doi.org/10.1002/dvg.22717

Schomburg, C., Turetzek, N., & Prpic, N.-M. (2020). Candidate gene screen for potential interaction partners and regulatory targets of the Hox gene labial in the spider *Parasteatoda tepidariorum*, 1–16. http://doi.org/10.1007/s00427-020-00656-7

Schoppmeier, M., & Damen, W. G. M. (2001). Double-stranded RNA interference in the spider Cupiennius salei : the role of Distal-less is evolutionarily conserved in arthropod appendage formation. *Development Genes and Evolution*, *211*(2), 76–82. http://doi.org/10.1007/s004270000121

Schwager, E. E., Pechmann, M., Feitosa, N. M., McGregor, A. P., & Damen, W. G. M. (2009). *hunchback* functions as a segmentation gene in the spider *Achaearanea tepidariorum*. *Current Biology : CB*, *19*(16), 1333–1340. http://doi.org/10.1016/j.cub.2009.06.061

Schwager, E. E., Schoppmeier, M., Pechmann, M., & Damen, W. G. (2007). Duplicated Hox genes in the spider *Cupiennius salei*. *Frontiers in Zoology*, *4*(1), 10–11. http://doi.org/10.1186/1742-9994-4-10

Schwager, E. E., Sharma, P. P., Clarke, T., Leite, D. J., Wierschin, T., Pechmann, M., et al. (2017). The house spider genome reveals an ancient whole-genome duplication during arachnid evolution. *BMC Biology*, *15*(1), 62. http://doi.org/10.1186/s12915-017-0399-x

Seiter, M., Lemell, P., Gredler, R., & Wolff, J. O. (2019). Strike kinematics in the whip spider Charon sp. (Amblypygi: Charontidae). *The Journal of Arachnology*, *47*(2), 260–7. http://doi.org/10.1636/JoA-S-18-089

Setton, E. V. W., & Sharma, P. P. (2018). Cooption of an appendage-patterning gene cassette in the head segmentation of arachnids. *Proceedings of the National Academy of Sciences*, *128*, 201720193–10. http://doi.org/10.1073/pnas.1720193115

Setton, E. V. W., March, L. E., Nolan, E. D., Jones, T. E., Cho, H., Wheeler, W. C., et al. (2017). Expression and function of *spineless* orthologs correlate with distal deutocerebral appendage morphology across Arthropoda. *Developmental Biology*, *430*(1), 224–236. http://doi.org/10.1016/j.ydbio.2017.07.016

Sharma, P. P., Kaluziak, S. T., Pérez-Porro, A. R., González, V. L., Hormiga, G., Wheeler, W. C., & Giribet, G. (2014a). Phylogenomic interrogation of Arachnida reveals systemic conflicts in phylogenetic signal. *Molecular Biology and Evolution*, *31*(11), 2963–2984. http://doi.org/10.1093/molbev/msu235

Sharma, P. P., Santiago, M. A., González-Santillán, E., Monod, L., & Wheeler, W. C. (2015a). Evidence of duplicated Hox genes in the most recent common ancestor of extant scorpions. *Evolution & Development*, *17*(6), 347–355. http://doi.org/10.1111/ede.12166

Sharma, P. P., Schwager, E. E., Extavour, C. G., & Giribet, G. (2012a). Evolution of the chelicera: a *dachshund* domain is retained in the deutocerebral appendage of Opiliones (Arthropoda, Chelicerata). *Evolution & Development*, *14*(6), 522–533.

http://doi.org/10.1111/ede.12005
Sharma, P. P., Schwager, E. E., Extavour, C. G., & Giribet, G. (2012b). Hox gene expression in the harvestman *Phalangium opilio* reveals divergent patterning of the chelicerate opisthosoma. *Evolution & Development*, *14*(5), 450–463. http://doi.org/10.1111/j.1525-142X.2012.00565.x
Sharma, P. P., Schwager, E. E., Extavour, C. G., & Wheeler, W. C. (2014b). Hox gene duplications correlate with posterior heteronomy in scorpions. *Proceedings. Biological Sciences*, *281*(1792), 20140661–20140661. http://doi.org/10.1098/rspb.2014.0661
Sharma, P. P., Schwager, E. E., Giribet, G., Jockusch, E. L., & Extavour, C. G. (2013). *Distal-less* and *dachshund* pattern both plesiomorphic and apomorphic structures in chelicerates: RNA interference in the harvestman *Phalangium opilio* (Opiliones). *Evolution & Development*, *15*(4), 228–242. http://doi.org/10.1111/ede.12029
Sharma, P. P., Tarazona, O. A., Lopez, D. H., Schwager, E. E., Cohn, M. J., Wheeler, W. C., & Extavour, C. G. (2015b). A conserved genetic mechanism specifies deutocerebral appendage identity in insects and arachnids. *Proceedings of the Royal Society B: Biological Sciences*, *282*(1808), 20150698–20150698. http://doi.org/10.1098/rspb.2015.0698
Shingate, P., Ravi, V., Prasad, A., Tay, B.-H., Garg, K. M., Chattopadhyay, B., et al. (2020). Chromosome-level assembly of the horseshoe crab genome provides insights into its genome evolution. *Nature Communications*, 1–13. http://doi.org/10.1038/s41467-020-16180-1
Sievers, F., Wilm, A., Dineen, D., Gibson, T. J., Karplus, K., Li, W., et al. (2011). Fast, scalable generation of high-quality protein multiple sequence alignments using Clustal Omega. *Molecular Systems Biology*, *7*, 1–6. http://doi.org/10.1038/msb.2011.75
Stollewerk, A., Schoppmeier, M., & Damen, W. G. M. (2003). Involvement of *Notch* and *Delta* genes in spider segmentation. *Nature*, *423*(6942), 863–865. http://doi.org/10.1038/nature01682
Struhl, G. (1981). A homoeotic mutation transforming leg to antenna in Drosophila. *Nature*, *292*(5824), 635–638.
Struhl, G. (1982). Genes controlling segmental specification in the Drosophila thorax. *Proceedings of the National Academy of Sciences*, *79*(23), 7380–7384. http://doi.org/10.1073/pnas.1717312115
Telford, M. J., & Thomas, R. H. (1998). Expression of homeobox genes shows chelicerate arthropods retain their deutocerebral segment. *Proceedings of the National Academy of Sciences*, *95*(18), 10671–10675. http://doi.org/10.1073/pnas.95.18.10671
The UniProt Consortium. (2018). UniProt: a worldwide hub of protein knowledge. *Nucleic Acids Research*, *47*(D1), D506–D515. http://doi.org/10.1093/nar/gky1049
Thomas, R. H., & Telford, M. J. (1999). Appendage development in embryos of the oribatid mite Archegozetes longisetosus (Acari, Oribatei, Trhypochthoniidae). *Acta Zoologica*, *80*(3), 193–200. http://doi.org/10.1046/j.1463-6395.1999.00016.x
Turetzek, N., Khadjeh, S., Schomburg, C., & Prpic, N.-M. (2017). Rapid diversification of homothorax expression patterns after gene duplication in spiders, 1–12. http://doi.org/10.1186/s12862-017-1013-0
Turetzek, N., Pechmann, M., Schomburg, C., Schneider, J., & Prpic, N.-M. (2015). Neofunctionalization of a Duplicate *dachshund* Gene Underlies the Evolution of a Novel Leg Segment in Arachnids. *Molecular Biology and Evolution*, *33*(1), 109–121. http://doi.org/10.1093/molbev/msv200
Wagner, G. P., Amemiya, C., & Ruddle, F. (2003). Hox cluster duplications and the opportunity for evolutionary novelties. *Proceedings of the National Academy of Sciences*, *100*(25), 14603–14606. http://doi.org/10.1073/pnas.2536656100

Waterhouse, R. M., Seppey, M., Simão, F. A., Manni, M., Ioannidis, P., Klioutchnikov, G., et al. (2017). BUSCO Applications from Quality Assessments to Gene Prediction and Phylogenomics. *Molecular Biology and Evolution*, *35*(3), 543–548. http://doi.org/10.1093/molbev/msx319

Weygoldt, P. (1969). Beobachtungen zur fortpflanzungsbiologie und zum verhalten der geißelspinne *Tarantula marginemaculata* C. L. Koch (Chelicerata, Amblypygi). *Zeitschrift Für Morphologie Der Tiere*, *64*(4), 338–360. http://doi.org/10.1007/BF00298640

Weygoldt, P. (1970). Lebenszyklus und postembryonale entwicklung der geibelspinne *Tarantula marginemaculata* C. L. Koch (Chelicerata, Amblypygi) im laboratorium. *Zeitschrift Für Morphologie Der Tiere*, *67*(1), 58–85. http://doi.org/10.1007/BF00280716

Weygoldt, P. (1975). Untersuchungen zur Embryologie und Morphologie der Geißelspinne *Tarantula marginemaculata* C. L. Koch (Arachnida, Amblypygi, Tarantulidae). *Zoomorphologie*, *82*, 137–199.

Weygoldt, P. (2000). Whip Spiders (Chelicerata: Amblypygi). Their Biology, Morphology and Systematics. Apollo Books.

Zhou, Y., Liang, Y., Yan, Q., Zhang, L., Chen, D., Ruan, L., et al. (2020). The draft genome of horseshoe crab *Tachypleus tridentatus* reveals its evolutionary scenario and well-developed innate immunity. *BMC Genomics*, *21*(1), 137–15. http://doi.org/10.1186/s12864-020-6488-1

Figure 1: *Phrynus marginemaculatus* as a model to study Amblypygi development. A: adult male *P. marginemaculatus*, dorsal view. B: adult female P. *marginemaculatus*, carrying protonymphs on the opisthosoma. The yellow ink is used to mark the females in the colony. C: dissecting dish made of plastic petri dish and foam. D: detail of an immobilized female ready to have the brood sac dissected. E: intact brood sac dissected from the female. F–G: deutembryo, in frontal, ventral and lateral view respectively. Scale bars: C: 1 cm (approximate); D: 5 mm (approximate); E: 1 mm; F–H: 500 µm.

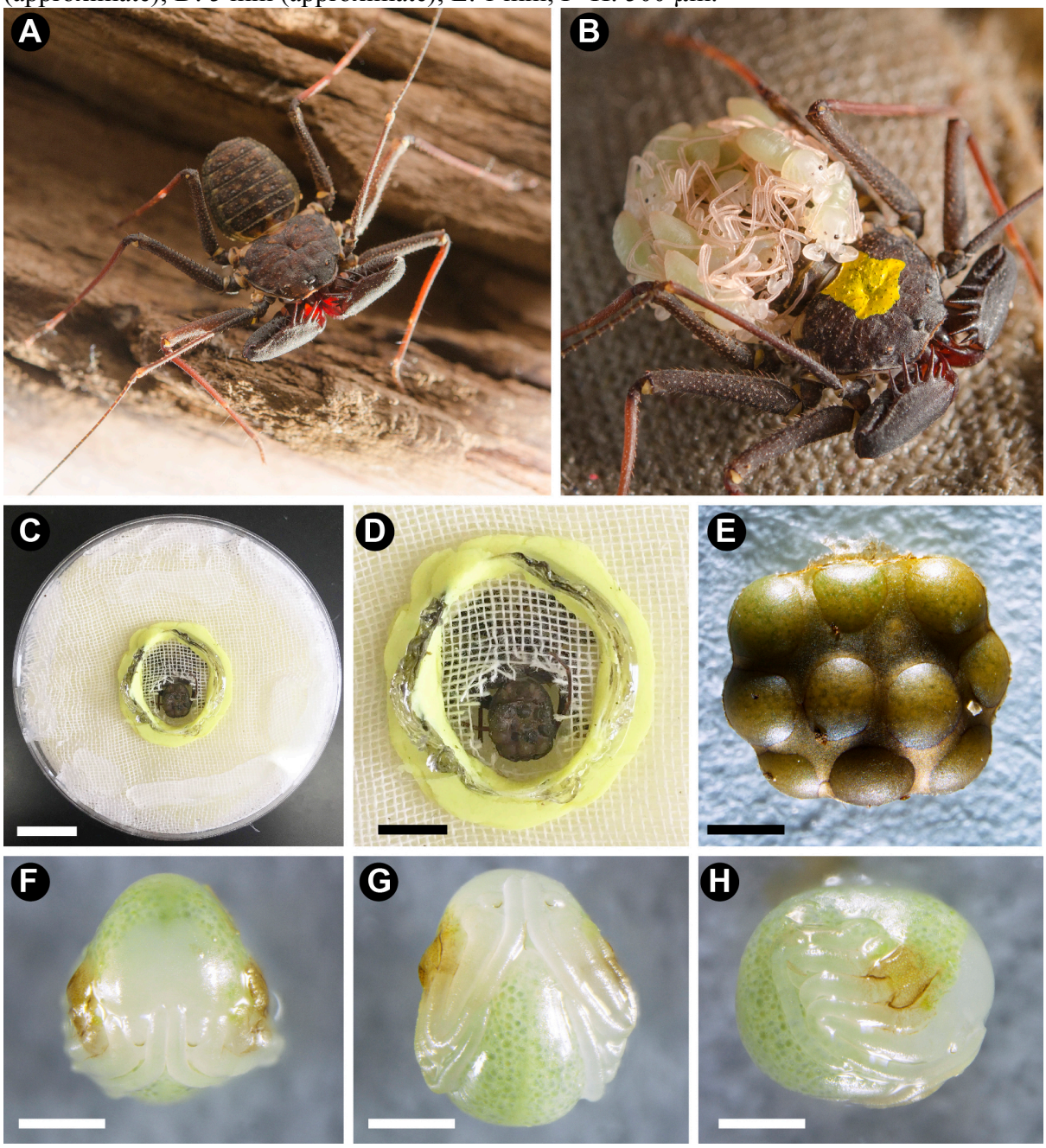

Figure 2: Overview of the embryonic development of *Phrynus marginemaculatus*. Z-stack automontage pictures of embryos imaged with nuclear staining (Hoechst) fluorescence. A–E: five embryonic stages, in ventral view, spanning the elongation of appendages, and showing germ band inversion and development of the ventral midline. F–H: head development, frontal view. F: undifferentiated head lobes. G: head lobe with neuron precursor cell invaginations. H: head lobes with anterior rim folding (semi-lunar grooves). I–K: opisthosomal development, posterior view. I: embryo with one opisthosomal segment. J: embryo with five opisthosomal segments. K: embryo ventral curved opisthosoma and most opisthosomal segments formed (number unclear). L–N: lateral organ formation and opisthosomal curving, lateral view. L: lateral organ as a undifferentiated bud proximal in leg II. M: lateral organ with a discreet "C" shape, and opisthosomal segments curved up. N: lateral organ in its final "kidney" shape, and opisthosoma curved ventrally. Ch: chelicera; Gz: growth zone; H: head lobe; Iv: neural precursor cell invagination; St: stomodeum. Scale bars: 500 µm.

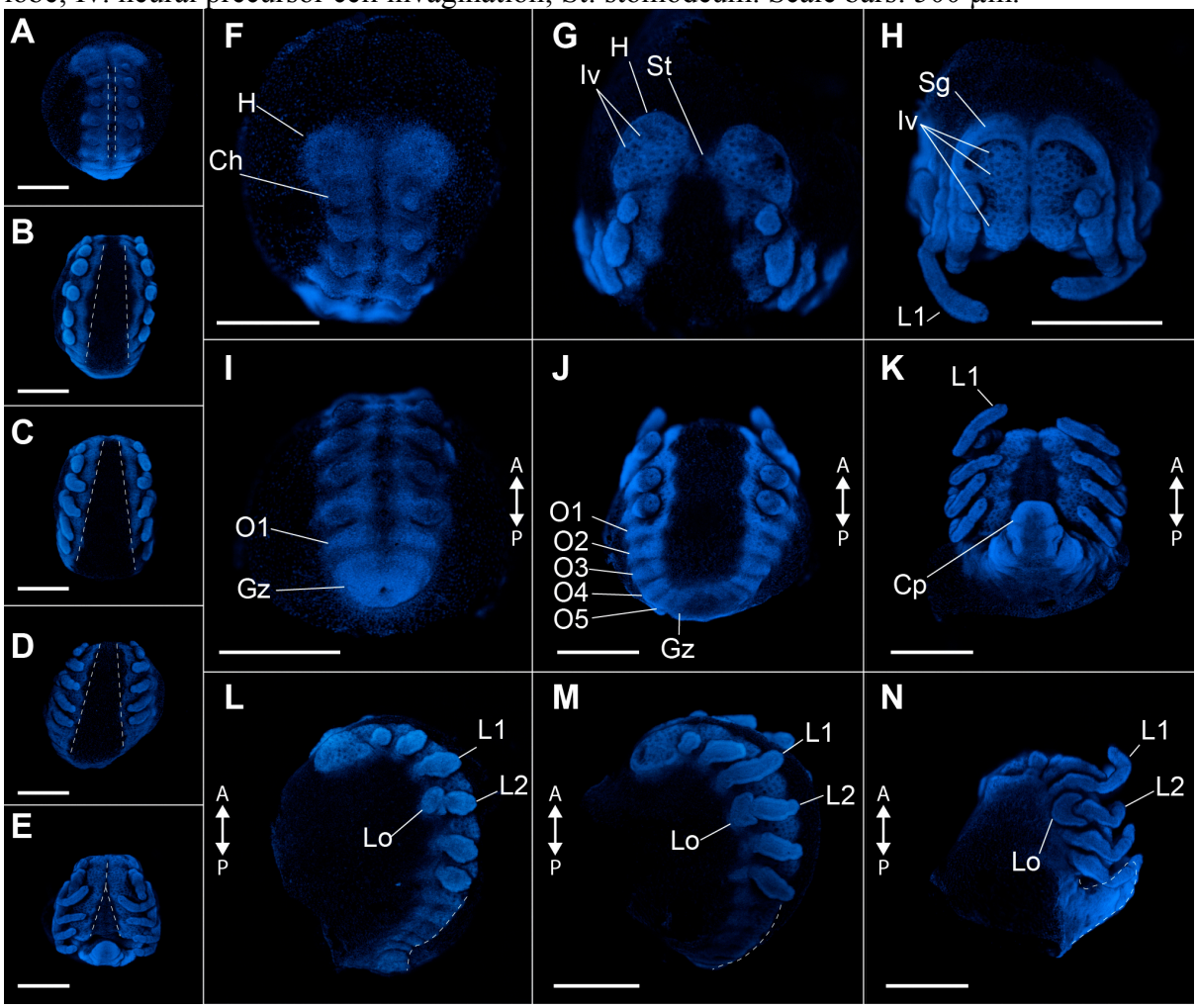

Figure 3: Hox gene duplications in *Phrynus marginemaculatus*. A: Schematic representation of the number of copies of each of the ten Hox genes in the selected arthropod terminals. Dotted square in *Phrynus* indicates lack of data not absence. Dotted square in *Parasteatoda Hox3* indicate questionable identity. Empty squares in *Parasteatoda* and *Tetranychus* indicate absence from the genome. B: Tree topology inferred from maximum likelihood analysis of a conserved region (73 amino acid characters) using the same terminals of the schematics (ln L = -3819.907). Numbers on the notes are ultrafast bootstrap resampling frequencies (only >80 shown). Species: *Phrynus marginemaculatus*; *Parasteatoda tepidariorum*; *Centruroides sculpturatus*; *Ixodes scapularis*; *Tetranychus urticae*; *Strigamia maritima*; *Drosophila melanogaster*; *Tribolium castaneum*. *lab*: *labial*; *pb*: *proboscipedia*/*maxillopedia*; *Hox3*: *Hox3*/*zerknullt*/*z2*; *Dfd*: *Deformed*; *Scr*: *Sex combs reduced*; *ftz*: *fushi tarazu*; *Antp*: *Antennapedia*/*prothorax-less*; *Ubx*: *Ultrabithorax*; *abdA*: *abdominal A*; *AbdB*: *Abdominal B*.

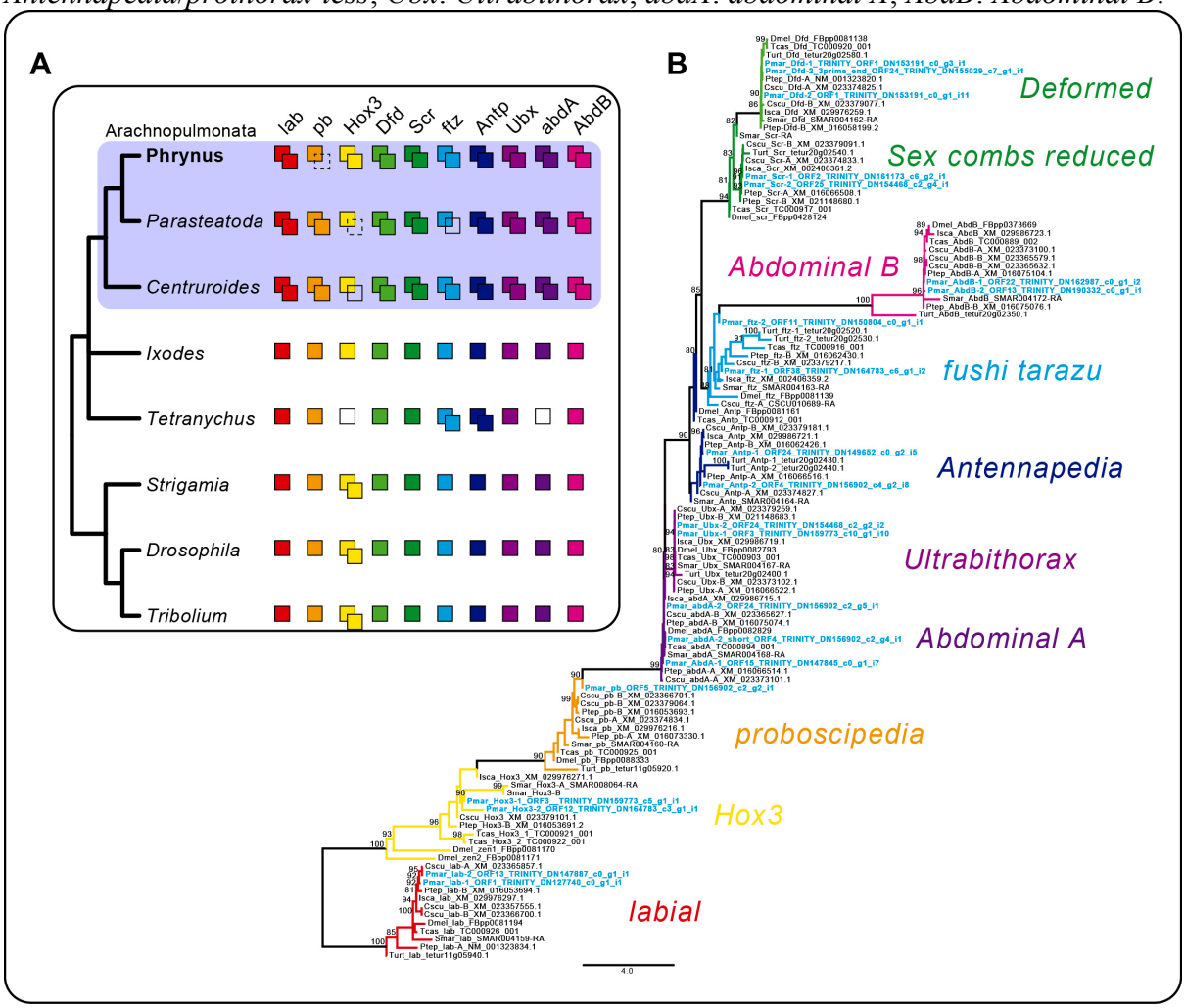

Figure 4: *Pmar-Distal-less* (*Pmar-Dll*) colorimetric in situ hybridization. Whole mount bright field images (Z-stack automontage) overlaid with nuclear staining (Hoechst). Ch: chelicera; Pp: pedipalp; L1–4: leg 1–4; A/P: anterior/posterior; dAEL: days after egg laying. Scale bars: 500 µm.

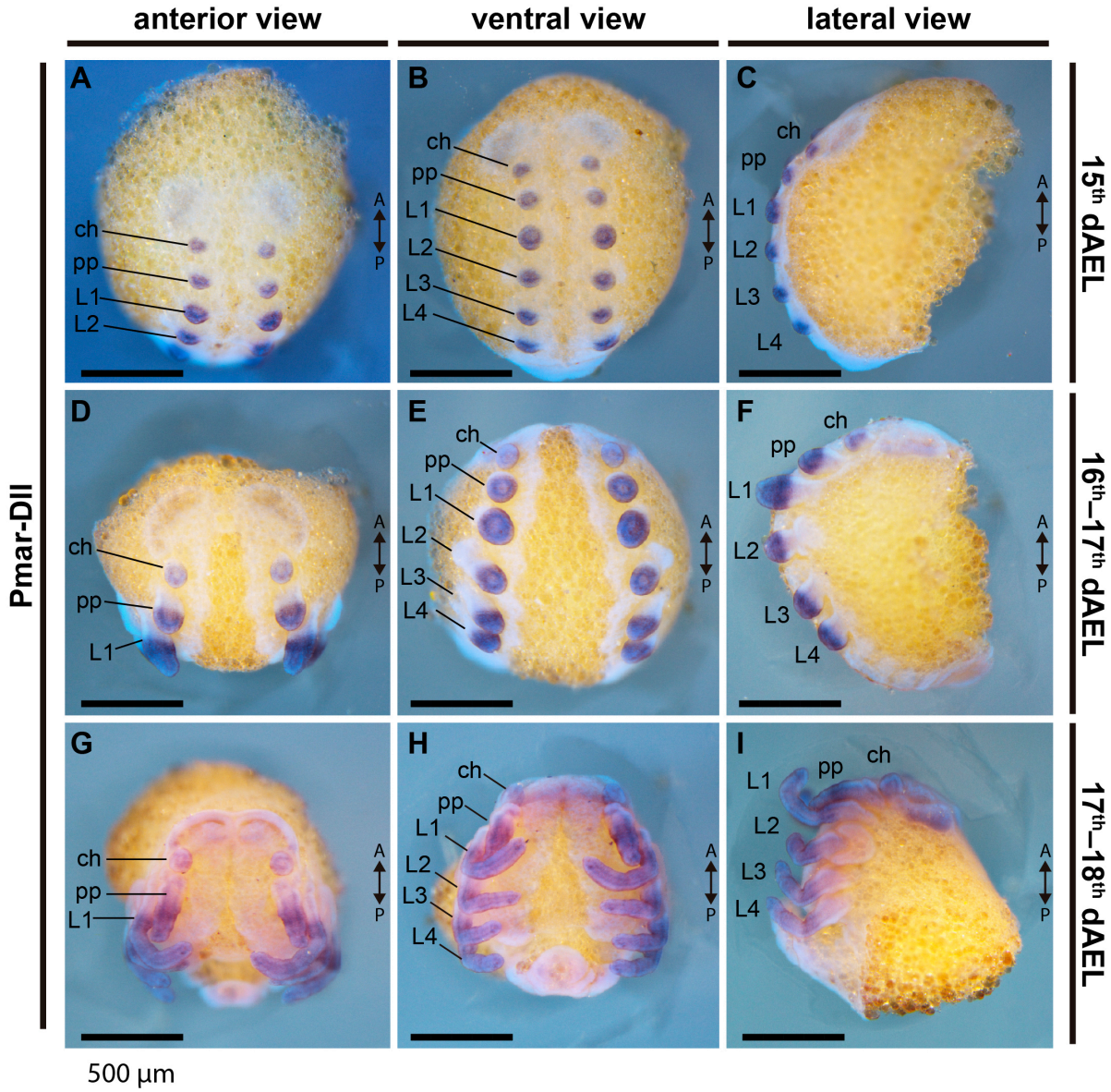

Figure 5: *Pmar-Distal-less* (*Pmar-Dll*) colorimetric in situ hybridization, appendage dissections in lateral view. Distal is to the left. A–F, G–L: bright field. A'–F', G'-L': nuclear staining (Hoechst), confocal Z-stack maximum projection. A–F: 16–17 dAEL embryo. G–L: 17-18 dAEL embryo. Distal is to the left. Ch: chelicera; Pp: pedipalp; L1–4: leg 1–4. Scale bar: 250µm.

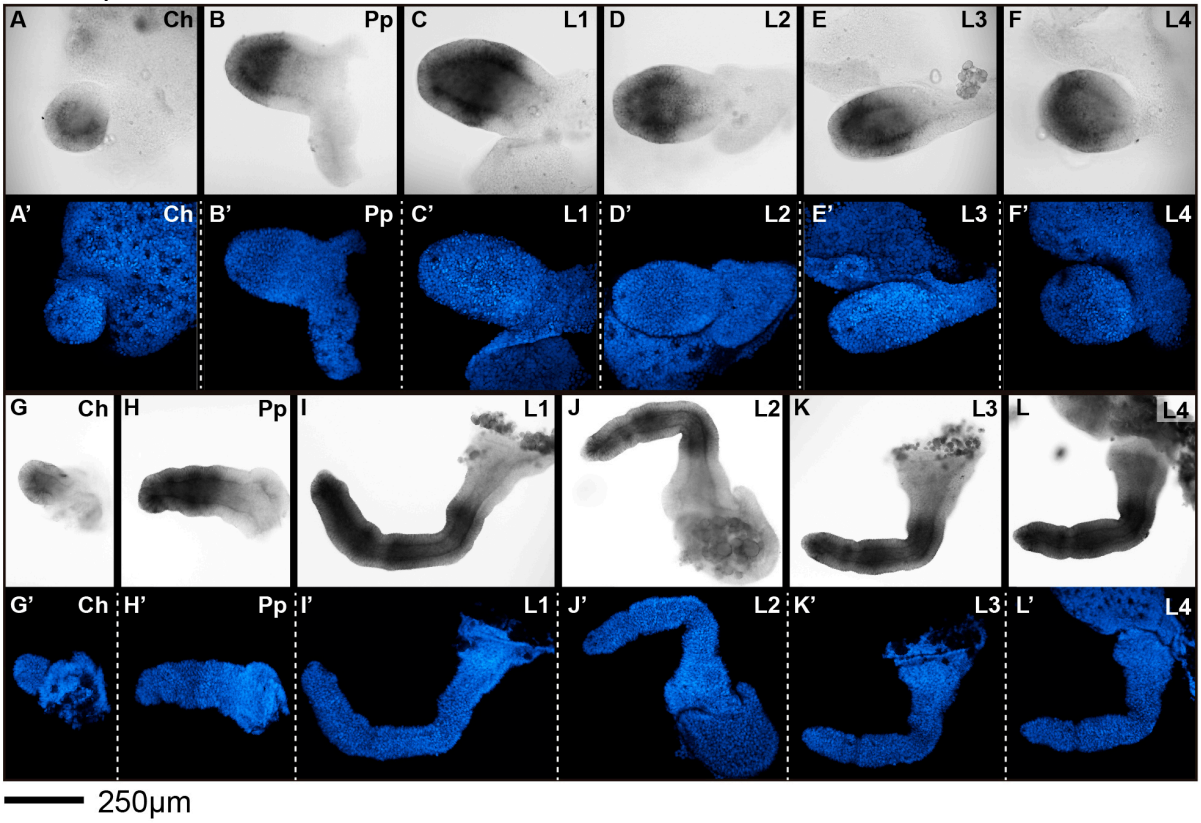

Figure 6: *Pmar-dachshund 1* (*Pmar-dac1*) (A–F) and *Pmar-dachshund 2* (*Pmar-dac2*) G–I) colorimetric in situ hybridization. Whole mount bright field images (Z-stack automontage) overlaid with nuclear staining (Hoechst). Ch: chelicera; Pp: pedipalp; L1–4: leg 1–4; Lo: lateral organ; A/P: anterior/posterior; arrowhead: expression domain; dAEL: days after egg laying. Scale bars: 500 µm.

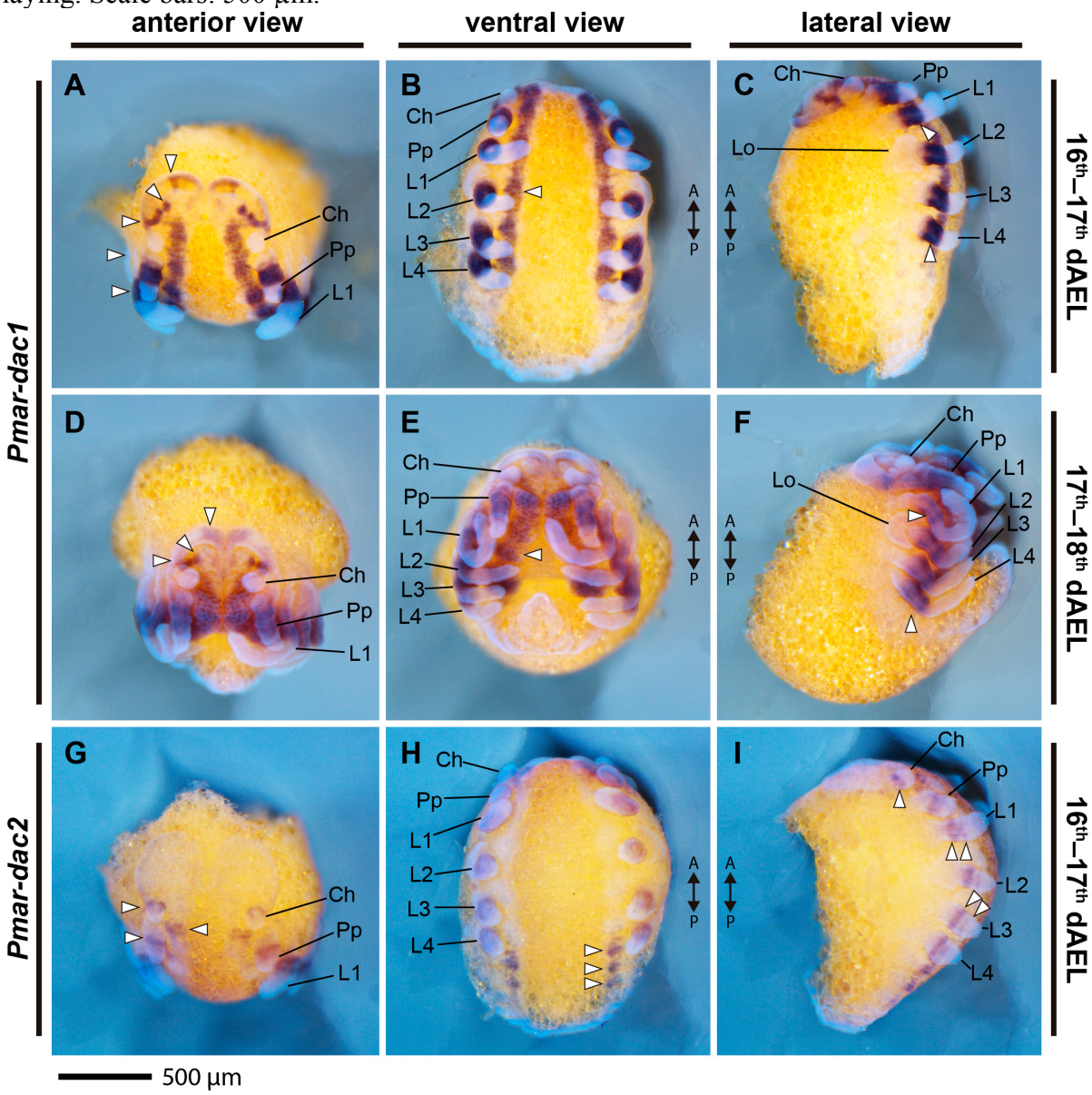

Figure 7: *Pmar-dachshund 1* (*Pmar-dac1*) (A–H) and *Pmar-dachshund 2* (*Pmar-dac2*) (I–L) colorimetric in situ hybridization, appendage dissections in lateral view. Distal is to the left. White arrowhead indicates discreet domains of expression. Asterisk in "E" marks expression from the lateral margin of the headlobe. Ch: chelicera; Pp: pedipalp; L1, 4: leg 1, 4. dAEL: days after egg laying. Scale bar: 200 µm.

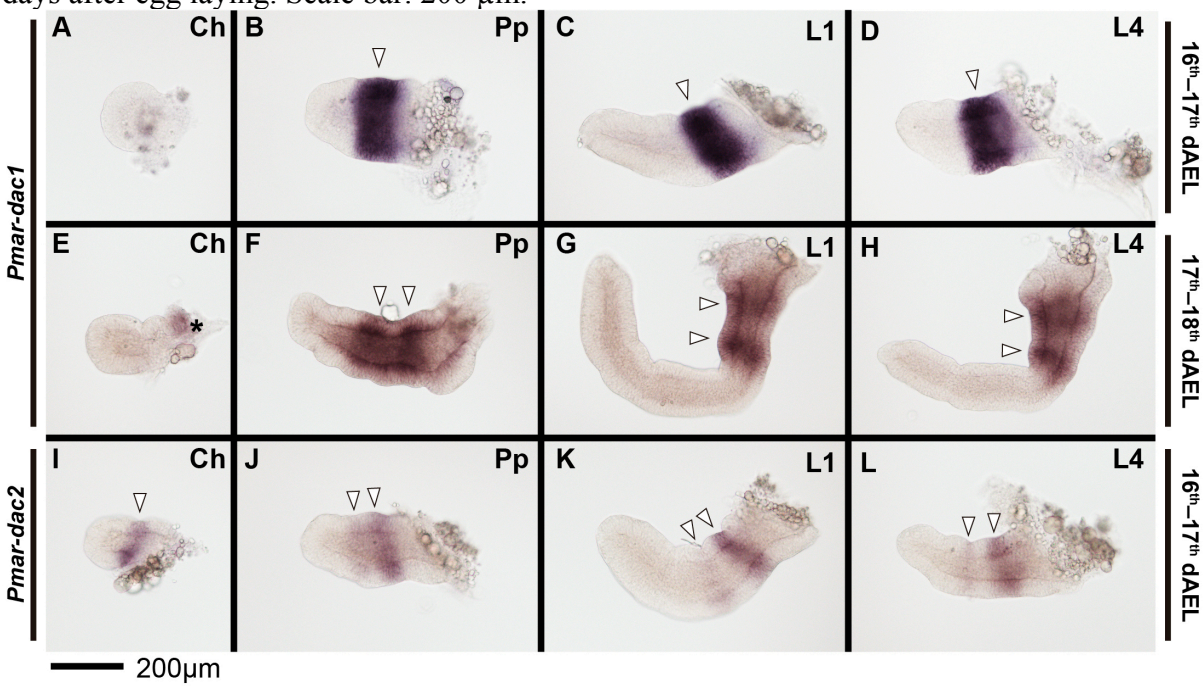

Figure 8: *Pmar-homothorax 1* (*Pmar-hth1*) (A–A') and *Pmar-homothorax 2* (*Pmar-hth2*) (B–B') colorimetric in situ hybridization, ventral view. A, B: whole mount bright field images (Z-stack automontage). A', B': nuclear staining (Hoechst) (Z-stack automontage). Ch: chelicera; Pp: pedipalp; L1–4: leg 1–4. A/P: anterior/posterior; arrowhead: expression domain; dAEL: days after egg laying. Scale bar: 500 µm.

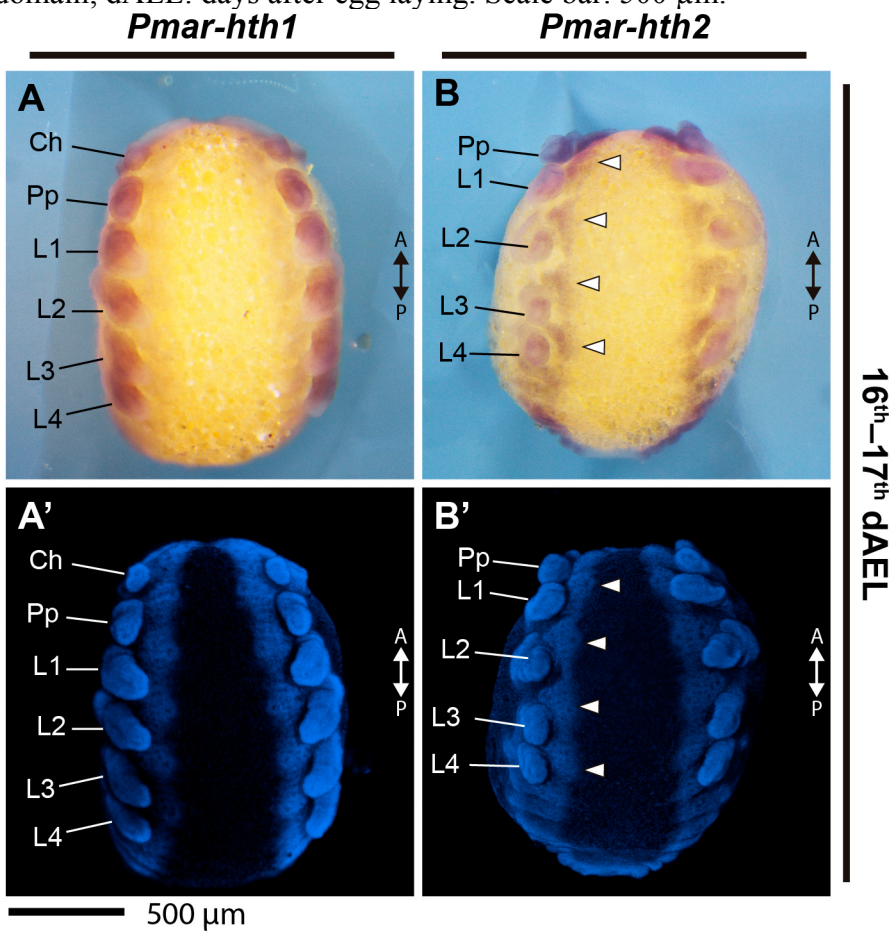

Figure 9: *Pmar-homothorax 1* (*Pmar-hth1*) (A–H) and *Pmar-homothorax 2* (*Pmar-hth2*) (I–L) colorimetric in situ hybridization, appendage dissections in lateral view. Distal is to the left. White arrowhead indicates discreet domains of expression. Ch: chelicera; Pp: pedipalp; L1, 4: leg 1, 4. dAEL: days after egg laying. Scale bar: 200 µm.

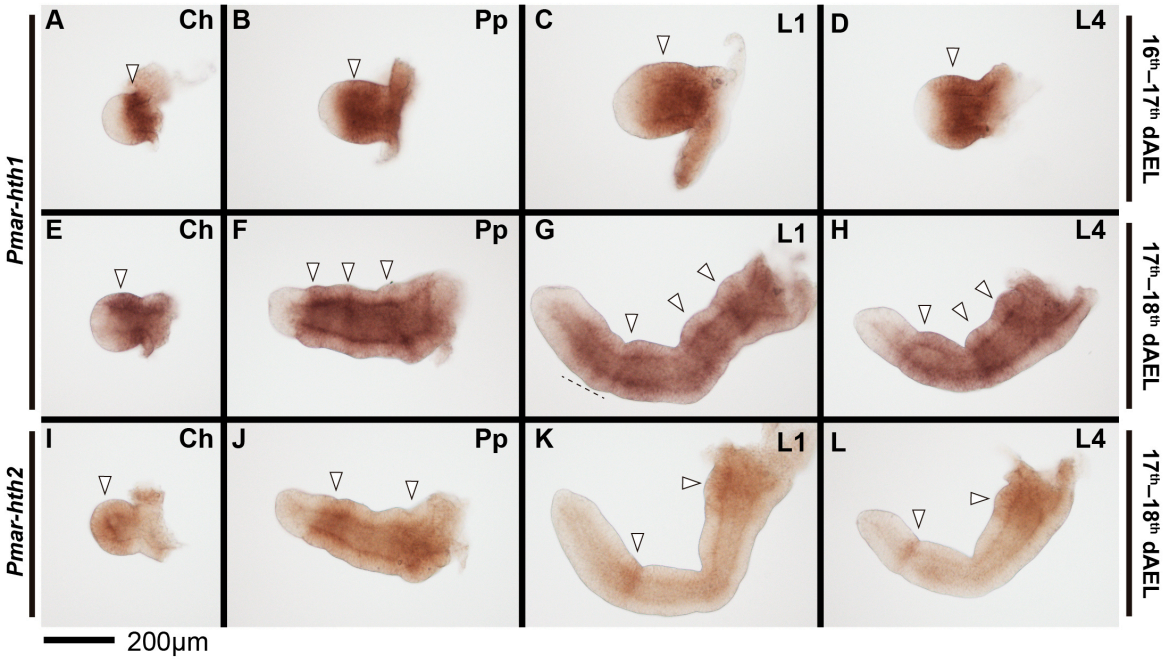

Figure S1: B: Tree topology inferred from maximum likelihood analysis of a conserved region (73 amino acid characters) (ln L = -3077.428) using the same terminals of Figure 1 and including the *Parasteatoda tepidariorum* putative *Hox3* paralog (red arrow). Numbers on the notes are ultrafast bootstrap resampling frequencies (only >80 shown). For abbreviations, see Table S1.

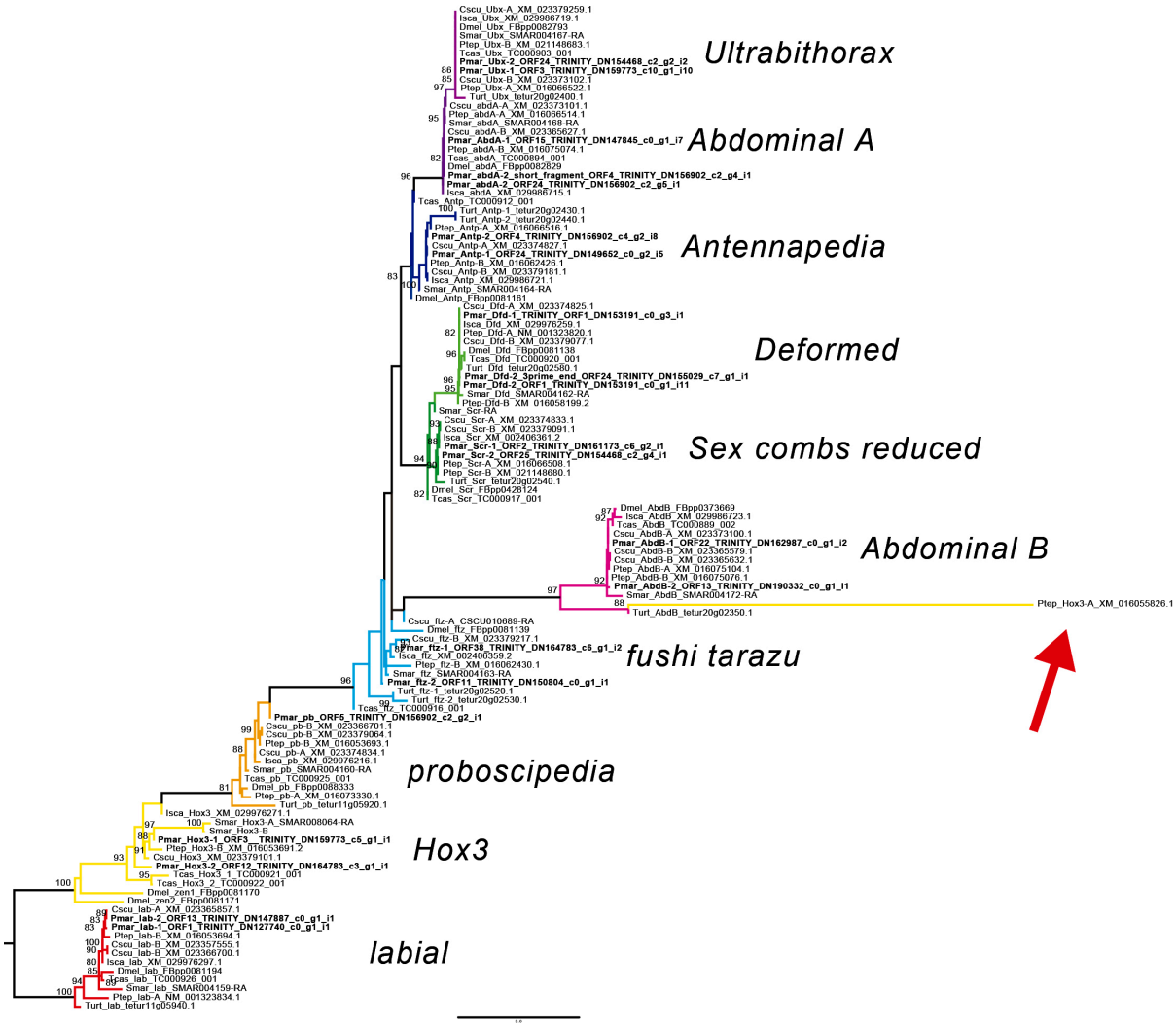

Figure S2: Tree topology of *Distal-less* (*Dll*) inferred from maximum likelihood analysis amino acid sequences (ln L = -15272.780). Numbers on the notes are ultrafast bootstrap resampling frequencies (only >80 shown). Accession numbers are available in Table S1. The terminal for the whip spider *Phrynus marginemaculatus Dll* ortholog is in boldface.

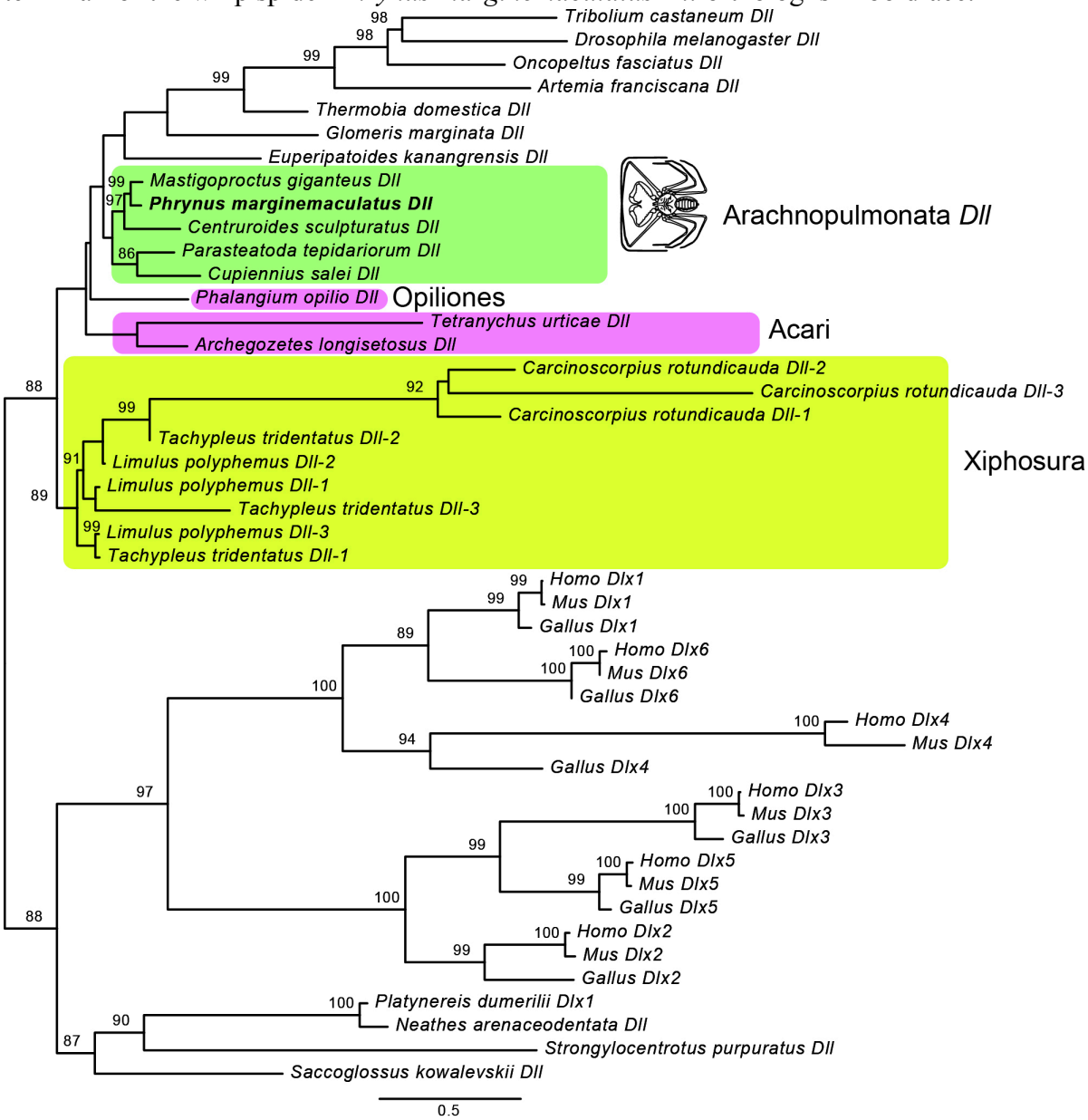

Figure S3: Tree topology of *dachshund* (*dac*) inferred from maximum likelihood analysis amino acid sequences (ln L = -21699.907). Numbers on the notes are ultrafast bootstrap resampling frequencies (only >80 shown). The terminals for the whip spider *Phrynus marginemaculatus Dll* orthologs are in boldface. The original protein alignment of all terminals (except *P. marginemaculatus*) is from Noland et al. 2020.

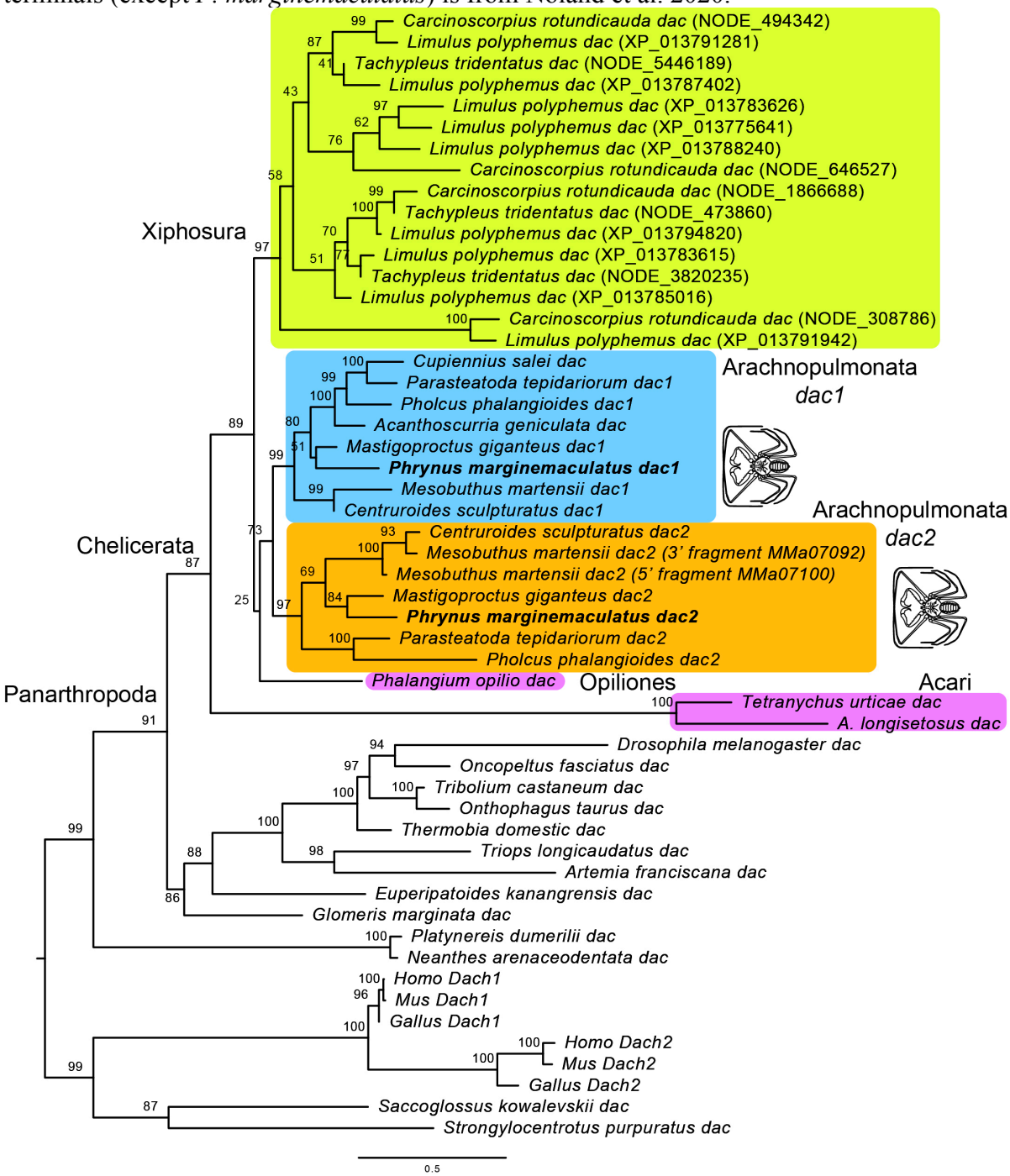

Figure S4: Tree topology of *homothorax* (*hth*) inferred from maximum likelihood analysis amino acid sequences (ln L = -10459.647). Numbers on the notes are ultrafast bootstrap resampling frequencies (only >80 shown). The terminals for the whip spider *Phrynus marginemaculatus hth* orthologs are in boldface. The original protein alignment of all terminals (except *P. marginemaculatus*) is from Noland et al. 2020.

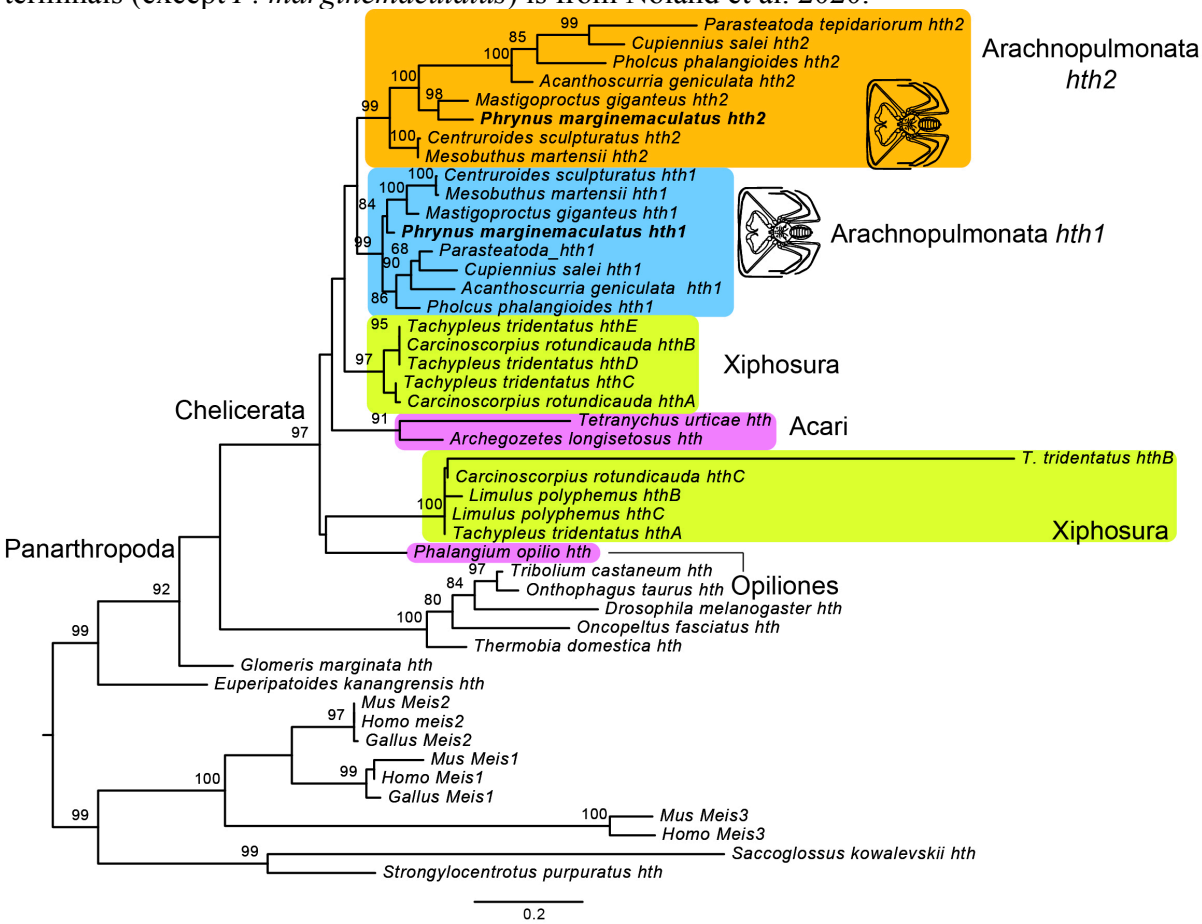

Table S1: List of species, accession numbers and abbreviations of terminals used in the phylogenetic analysis of Hox genes, *Distal-less*, *dachshund* and *homothorax* homologs.

Table S2: List of primers for *Pmar-Dll*, *Pmar-dac1/2*, *Pmar hth1/2*, and cloned fragments for *Pmar-Dll*.